Influence of Frequency on Compaction of Sand in Small-Scale Tests

Carl Wersäll

Preface

This project was carried out between February 2011 and November 2013 at the Division of Soil and Rock Mechanics, Department of Civil and Architectural Engineering, Royal Institute of Technology (KTH) in Stockholm, Sweden. Supervisor was Prof. Stefan Larsson at KTH and assistant supervisor was Dr. Nils Rydén at the Faculty of Engineering, Lund University (LTH) and PEAB AB.

Stockholm, November 2013

Carl Wersäll

Abstract

Vibratory rollers are commonly used for compaction of embankments and landfills. In a majority of large construction projects, this activity constitutes a significant part of the project cost and causes considerable emissions. Thus, by improving the compaction efficiency, the construction industry would reduce costs and environmental impact. In recent years, rollers have been significantly improved in regard to engine efficiency, control systems, safety and driver comfort. However, very little progress has been made in compaction effectiveness. While the compaction procedure (e.g. layer thickness and number of passes) has been optimized over the years, the process in which the machine compacts the underlying soil is essentially identical to the situation in the 1970s.

This research project investigates the influence of one crucial parameter, namely vibration frequency of the drum, which normally is a fixed roller parameter. Frequency is essential in all dynamic systems but its influence on the compaction efficiency has not been studied since the early days of soil compaction. Since laboratory and field equipment, measurement systems and analysis techniques at the time were not as developed as they are today, no explicit conclusion was drawn. Frequency-variable oscillators, digital sensors and computer-based analysis now provide possibilities to accurately study this concept in detail.

In order to examine the influence of vibration frequency on the compaction of granular soil, small-scale tests were conducted under varying conditions. A vertically oscillating plate was placed on a sand bed contained in a test box. The experiments were carried out in laboratory conditions to maximize controllability. The first test setup utilized an electro-dynamic oscillator where dynamic quantities, such as frequency and particle velocity amplitude, could be varied in real-time. The second test setup included two counter-rotating eccentric mass oscillators, where tests were conducted at discrete frequencies. This type of oscillator has a force amplitude that is governed by frequency.

The main objectives of the tests were to determine the optimal compaction frequency and whether resonance can be utilized to improve compaction efficiency. Results showed that resonance had a major influence in the electro-dynamic oscillator tests, where the applied force amplitude is low, and the optimal compaction frequency is the resonant frequency under these circumstances. In the rotating mass oscillator tests, where a high force was applied to the plate, resonant amplification was present but not as pronounced. Since force increase with frequency, the optimal frequency to obtain the highest degree of compaction is very large. In a practical regard, however, frequency should be kept as low as possible to minimize machine wear and emissions while still achieving a sufficient compaction of the soil. Considering the practical issues, it is proposed that surface compactors should operate slightly above the resonant frequency. However, the applicability to vibratory rollers must be confirmed in full-scale tests.

The thesis also presents an iterative method to calculate the frequency response of a vibrating plate, incorporating strain-dependent soil properties. Calculated dynamic quantities are compared to measured values, confirming that the method accurately predicts the response.

Sammanfattning

Vibrationsvältar används normalt vid packning av fyllningar och väg- och järnvägsbankar. I merparten av alla anläggningsprojekt utgör denna aktivitet en stor del av projektkostnaden och orsakar betydande utsläpp. Genom att effektivisera packningsprocessen skulle därför byggbranschen kunna minska kostnader och miljöpåverkan. Under senare år har vältar utvecklats med avseende på motorer, kontrollsystem, säkerhet och förarkomfort. Dock har mycket lite utveckling skett av packningseffektiviteten. Medan packningsförfarandet (t.ex. lagertjocklek och antal överfarter) har optimerats under åren är processen i vilken maskinen packar underliggande jord identisk med situationen på 1970-talet.

Detta forskningsprojekt undersöker inflytandet av en grundläggande parameter, nämligen valsens vibrationsfrekvens, vilken vanligtvis är en icke-variabel vältparameter. Frekvensen är av avgörande betydelse i alla dynamiska system men dess inflytande på packningseffektiviteten har inte undersökts sedan jordpackningens barndom. Eftersom dåtidens laboratorie- och fältutrustning, mätsystem och analysförfarande inte var så utvecklade som de är idag uppnåddes inga konkreta slutsatser. Frekvensvariabla vibratorer, digitala mätsystem och datorbaserad utvärdering tillhandahåller nu nya möjligheter för att studera detta koncept i detalj.

För att undersöka frekvensens betydelse vid packning av grovkornig jord utfördes småskaleförsök under varierande förhållanden. En vertikalt vibrerande platta placerades på ett sandlager inneslutet i en försökslåda. Experimenten utfördes i laboratoriemiljö för att maximera kontrollerbarheten. I den första försöksuppsättningen användes en elektrodynamisk vibrator där dynamiska kvantiteter, såsom frekvens och svängningshastighetsamplitud, kunde varieras i realtid. Den andra försöksuppsättningen innefattade två vibratorer med motriktade roterande excentermassor och försöken utfördes vid diskreta frekvenser. Denna typ av vibrator ger upphov till en kraftamplitud som är frekvensberoende.

Försökens huvudsakliga syfte var att fastställa den optimala packningsfrekvensen och undersöka om resonans kan godtyckliggöras för att förbättra packningseffektiviteten. Resultaten visade att resonans hade en avgörande betydelse i försöken med den elektrodynamiska vibratorn, där kraftamplituden är låg, och den optimala packningsfrekvensen är under dessa förutsättningar resonansfrekvensen. Även i försöken med roterande excentermassor, där en hög kraftamplitud anbringades plattan, uppstod resonansförstärkning, dock ej lika markant. Eftersom kraft ökar med frekvens är den optimala packningsfrekvensen mycket hög. I praktiken bör dock frekvensen hållas så låg som möjligt för att minimera maskinslitage och utsläpp, och samtidigt uppnå en tillräcklig packning av jorden. Med hänsyn taget till de praktiska aspekterna föreslås att ytpackningsdon bör arbeta något över resonansfrekvensen. Dock måste tillämpbarheten för vibrationsvältar bekräftas i fullskaleförsök.

Avhandlingen presenterar också en iterativ metod för att beräkna frekvensresponsen av en vibrerande platta, som tar hänsyn till töjningsberoende jordegenskaper. Beräknade dynamiska kvantiteter jämförs med uppmätta värden och bekräftar att metoden framgångsrikt kan förutsäga responsen.

List of Publications

The following papers are appended to the thesis:

Paper I

Wersäll, C. and Larsson, S., 2013, "Small-Scale Testing of Frequency-Dependent Compaction of Sand Using a Vertically Vibrating Plate," *Geotechnical Testing Journal*, Vol. 36, No. 3, pp. 1-10.

Wersäll conducted the experiments, performed the analysis and wrote the paper. Larsson supervised the work and assisted in interpreting the results and writing the paper.

Paper II

Wersäll, C., Larsson, S., Rydén, N. and Nordfelt, I., 2013, Frequency Variable Surface Compaction of Sand Using Rotating Mass Oscillators, Submitted to Geotechnical Testing Journal in November 2013.

Wersäll conducted the experiments, performed the analysis and wrote the paper. Larsson supervised the work and assisted in writing the paper. Rydén and Nordfelt assisted in interpreting the results and provided valuable comments on planning the tests and writing the paper.

x

Contents

List of Symbols

A	Dimensionless stiffness coefficient
B_z	Mass ratio
F	Force
F_0	Force amplitude
F_c	Force in damper element
F_k	Force in spring element
F_m	Force in mass element
G	Shear modulus
G_{max}	Small-strain shear modulus
L_ε	Length of strained element
M	Dynamic magnification factor for constant force
M'	Dynamic magnification factor for rotating mass oscillators
N	Number of loading cycles
OCR	Overconsolidation ratio
P	Power
P_a	Atmospheric pressure
PI	Plasticity index
S	Settlement of the plate
W_c	Energy consumed in one cycle
a	Acceleration
a_0	Acceleration amplitude
c	Damping coefficient
c_{cr}	Critical damping coefficient
c_R	Rayleigh wave speed
c_S	Shear wave speed
e	Eccentricity
e	Void ratio
d_{10}	Diameter for 10 % passing
d_{60}	Diameter for 60 % passing
f	Frequency
f_r	Resonant frequency
g_{RMS}	RMS value of function g
k	Spring stiffness
k	Exponent depending on PI
m	Mass
m_0	Mass of foundation
m_e	Eccentric mass
$m_e e$	Eccentric moment
m_s	Apparent mass

n	Exponent depending on stress state
r_0	Footing radius
t	Time
u	Displacement
u_0	Displacement amplitude
u_A	Nominal displacement amplitude
u_{LVDT}	Settlement of the plate
v	Velocity
v_0	Velocity amplitude
v_{LVDT}	Displacement velocity of the plate
w	Water content
ΔV_c	Compacted volume
ΔV_d	Displaced volume
α	Empirical factor depending on PI
β	Dimensionless frequency
β	Empirical exponent depending on PI
γ	Shear strain
γ_r	Reference shear strain
ε	Compressive strain
ζ	Damping ratio
ζ_{max}	Maximum damping ratio
ν	Poisson's ratio
ρ	Mass density
$\sigma'_0{}^n$	Effective isotropic confining pressure
τ	Shear stress
ω	Circular frequency
ω_n	Circular natural frequency

1   INTRODUCTION

1.1   Background

Soil compaction is the most common ground improvement method and is often necessary to reduce settlement, increase stability and stiffness of the subgrade, control swelling and creep, lower the risk of liquefaction and decrease the permeability. It implies densification of the soil by reducing its pore volume. In granular soil, this is normally achieved by vibration or impact, producing stress-waves that rearrange the soil particles into a denser state. In construction of embankments and landfills, soil is placed in layers and compacted using vibratory roller (Figure 1). This process is time-consuming and normally constitutes a significant part of the project cost as well as giving rise to considerable emissions. It is thus in the interest of the industry to improve the compaction efficiency and reduce the time for this activity.

As vibratory rollers became popular around the 1950s, the optimal compaction procedure became a topic of research. One fundamental property that was investigated was the compaction frequency. All rollers operate with rotating eccentric mass oscillators that produce increasing force amplitude with frequency. However, all dynamic systems have a resonant frequency where vibrations are amplified. For roller compaction, this is within the operating frequency of the roller and taking advantage of this amplification might therefore be feasible. Several studies were conducted in the early years of this research field (especially in the 1950s and 1960s), with varying results. However, the available compaction equipment, measurement systems and evaluation techniques at the time were far from what they are today. Frequency was normally varied by adjusting the speed of the engine, which is a crude method for frequency variation. Since digital sensors or computers were not

Figure 1. Vibratory roller (courtesy of Dynapac Compaction Equipment AB).

available, results were difficult to interpret. Furthermore, there are many aspects that affect the results, not all of which were known at the time. First of all, a dynamic system behaves very differently below, close to or above resonance. Hence, it is important to be aware of the compaction frequency in relation to the resonant frequency. The acceleration amplitude is also of great importance. Several authors have found that compaction should be performed at accelerations above 1 g to be effective (D'Appolonia et al. 1969; Dobry & Whitman 1973). There are several other aspects, such as dynamic-to-static load ratio, shape of the contact surface and soil properties. Due to the complexity of the problem, the early studies had varying conclusions.

The first to propose a compactor, utilizing frequency to obtain the maximum degree of compaction was Hertwig (1936). Tschebotarioff & McAlpin (1947) concluded that the subsidence of a piston, vibrating on the soil was independent of frequency as long as the total number of cycles was constant. However, the frequency in those tests was very low, less than 20 Hz. Bernhard (1952) conducted laboratory tests with variable frequency and constant force, obtaining a more efficient compaction at the resonant frequency. Converse (1953) conducted field compaction tests of sand and also concluded that resonance could be utilized. Forssblad (1965) highlighted that in the tests by Bernhard and Converse the dynamic load was only in the same order of magnitude as the static weight and argued that the results could not be compared to roller compaction. Several other authors found a correlation between resonance and increased compaction efficiency (Johnson & Sallberg 1960; Lorenz 1960). Forssblad (1965) argued that the increase in force amplitude with frequency would be too significant for the resonant amplification to influence the compaction effect and that the technical difficulties for utilizing resonance would exceed the practical advantages. Thus, there was no agreement among researchers on whether resonant amplification could be used to improve roller compaction. There was, however, one conclusion on with the community agreed, namely that effective compaction must be performed above the resonant frequency.

There have been many attempts to model the roller behavior by mathematical or numerical methods. Yoo & Selig (1979) presented a lumped-parameter model that formed the basis for most subsequent models of roller behavior. These studies have mainly been conducted for the purpose of continuous compaction control and intelligent compaction (e.g., Forssblad 1980; Thurner & Sandström 1980; Adam 1996; Anderegg & Kaufmann 2004; Mooney & Rinehart 2009; Facas et al. 2011). Modeling the dynamic behavior of compaction equipment is complicated by the fact that soil shows very nonlinear stress-strain behavior. Most models do not take this into account. However, Susante & Mooney (2008) developed a model that includes nonlinear soil stress-strain behavior, calculating the response in time domain.

In the 1970s, computer programs using an equivalent linear approach to determine the nonlinear seismic response during earthquakes, such as SHAKE (Schnabel et al. 1972), became popular. These programs apply an iterative procedure to determine the nonlinear response of a transient time history. As finite element and other numerical methods were introduced, these became dominating in calculating the nonlinear response. However, numerical methods are time-consuming and require skilled operators to be reliable. Thus, equivalent linear methods are still useful but there has hardly been any development of these concepts in recent years. No one has previously used this approach

for calculating the nonlinear response of an oscillating foundation (such as surface compaction equipment) on soil with strain-dependent properties.

1.2 Objectives

This research project aims at determining the optimal compaction frequency of vibratory rollers and to investigate whether resonance in the roller-soil system can be utilized for increasing the compaction efficiency. As a first step, the fundamental dynamic behavior during frequency-variable compaction is studied. The main objective of this thesis is to investigate the influence of frequency on the compaction of sand in small-scale tests. These are conducted under varying conditions to quantify the effect of, not only frequency, but also type of oscillator, dynamic load and soil water content. The small-scale tests form a basis for full-scale tests using vibratory roller.

Another objective is to develop an equivalent linear calculation procedure that can be performed in frequency domain. These calculations are compared to results of the small-scale tests.

1.3 Outline of Thesis

This thesis consists of an introductory part and two appended paper, one published in a peer-reviewed journal and the other submitted to the same journal. The introductory part is intended as an introduction and a complement to the appended papers. It contains background information, summary of the main findings and further development of some concepts that are included in the papers.

Chapter 2 describes the fundamentals of dynamic single degree of freedom systems and vertically oscillating foundations. The linear equivalent calculation procedure developed in Paper II is described in detail. All necessary background information for understanding of this procedure is provided.

Chapter 3 is a description of the small-scale tests. Since the tests are described thoroughly in the papers, this chapter summarizes briefly the test setups and provides additional photographs of the equipment. The test results of the two papers are summarized and discussed in relation to each other.

Chapter 4 contains a summary of the appended papers.

Chapter 5 provides the main conclusions of the thesis and papers and suggests further research.

INTRODUCTION

2 OSCILLATING FOUNDATIONS ON SOFTENING SOIL

Studies on vibrating foundations began with the objective to analyze ground vibrations from rotating machinery founded on the ground surface. This has become the basis for dynamic soil-structure interaction analysis, including many more applications than just rotating machinery, such as wind turbines and bridge abutments subjected to traffic load. This chapter describes how basic equations for vibrating foundations can be combined with empirical knowledge for nonlinear stress-strain behavior of soil to predict the dynamic response of vibrating foundations on softening soil. Since this thesis deals with vertical oscillations on granular soil, other oscillatory motions or plastic soils are not treated herein. For other vibration modes, such as rocking or horizontal oscillation, reference is made to Richart et al. (1970) and Gazetas (1983).

2.1 Single Degree of Freedom Systems

The dynamic behavior of a vertically oscillating foundation can be estimated by analyzing a single degree of freedom (SDOF) system consisting of a mass, a dashpot and a spring, where the force in these three components are proportional to acceleration, velocity and displacement, respectively. The forces in each element (F_m, F_c and F_k) are determined by Equations 1 to 3.

$$F_m = ma \tag{1}$$

$$F_c = cv \tag{2}$$

$$F_k = ku \tag{3}$$

where m is mass, a is acceleration, c is damping coefficient, v is vibration velocity, k is spring stiffness and u is displacement. Since the velocity is given by $v = \frac{du}{dt}$ and the acceleration is given by $a = \frac{d^2u}{dt^2}$, and since all forces need to be in equilibrium, a SDOF system can be described by the second order differential equation presented in Equation 4.

$$m\frac{d^2u}{dt^2} + c\frac{du}{dt} + ku = F(t) \tag{4}$$

where $F(t)$ is the externally applied force. The system may be either under-damped, critically damped or over-damped depending on if the damping coefficient is less than, equal to or larger than the critical damping coefficient c_{cr}. The ratio between these is denoted damping ratio, ζ, and is shown in Equation 5.

$$\zeta = \frac{c}{c_{cr}} = \frac{c}{2\sqrt{km}} \tag{5}$$

All dynamic systems have one or several natural frequencies. The circular natural frequency, ω_n, of a SDOF system is calculated by Equation 6.

$$\omega_n = \sqrt{\frac{k}{m}} \tag{6}$$

It is convenient to express frequency normalized by the natural frequency, the so-called dimensionless frequency, β, as shown in Equation 7.

$$\beta = \frac{\omega}{\omega_n} \tag{7}$$

where ω is the circular frequency. For a harmonic external load, the solution to Equation 4 may then be expressed by Equation 8.

$$u_0 = \frac{F_0}{k} \frac{1}{\sqrt{(1-\beta^2)^2 + (2\zeta\beta)^2}} \tag{8}$$

where u_0 is displacement amplitude and F_0 is force amplitude. The dynamic displacement in relation to the displacement that would be obtained from static loading by the same force is called dynamic magnification factor. It is calculated by Equation 9 and shown in Figure 2 for different values of the damping ratio.

$$M = \frac{u_0}{F_0/k} = \frac{1}{\sqrt{(1-\beta^2)^2 + (2\zeta\beta)^2}} \tag{9}$$

When the frequency approaches zero, the magnification factor approaches unity. As the excitation frequency approaches the natural frequency, the dynamic response is significantly magnified. The
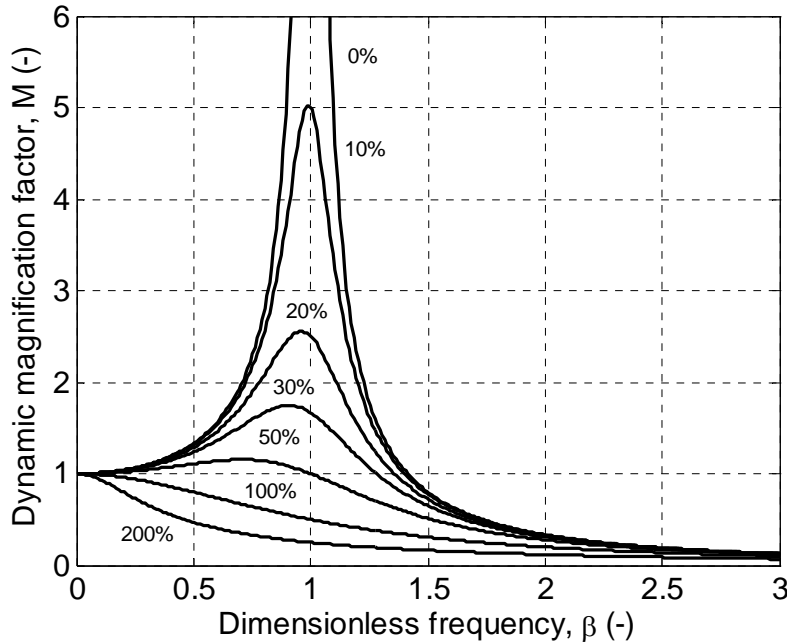

Figure 2. Dynamic magnification factor for constant force and different damping ratios.

frequency where maximum magnification occurs is the resonant frequency, which is equal to the natural frequency when damping is zero and slightly lower as the damping ratio becomes larger. When the frequency is increased above resonance, the magnification factor (and thus the displacement amplitude) decreases and approaches zero for large frequencies. If the damping ratio is zero, the resonant amplification is infinite. This is an unrealistic case as there are no real systems without damping. However, for a damping ratio of 10 %, which represents quite high damping, the resonant amplification is still as high as 5 times the static value. The damping ratios of 20-30 % shown in the figure are uncommon but can occur for example during large strain in soil, as will be discussed below.

The magnification factor shown in Figure 2 is for the case where the applied force amplitude is constant with frequency. If the load would be produced by rotating mass oscillators, force amplitude would increase rapidly with frequency according to Equation 10.

$$F_0 = m_e e \omega^2$$ (10)

where m_e is the eccentric mass and e is the eccentricity. The nominal displacement amplitude of a rotating mass oscillator, u_A, is given by Equation 11.

$$u_A = \frac{m_e e}{m}$$ (11)

Details regarding the properties of rotating mass oscillators can be found in, for example, Forssblad (1981). By applying Equations 6 and 10 and 11, Equation 8 may be rewritten as Equation 12 with a corresponding dynamic magnification factor for rotating mass oscillators, M', given by Equation 13.

$$u_0 = u_A \frac{\beta^2}{\sqrt{(1 - \beta^2)^2 + (2\zeta\beta)^2}}$$ (12)

$$M' = \frac{u_0}{u_A} = \frac{\beta^2}{\sqrt{(1 - \beta^2)^2 + (2\zeta\beta)^2}}$$ (13)

The magnification factor is shown in Figure 3. Since the dynamic force is generated by the rotating masses, there is no or very little dynamic displacement when the frequency is zero or close to zero. Thus the magnification factor approaches zero when the frequency goes toward zero. The behavior around resonance is similar to the case with constant force, except from the resonant frequency being slightly larger than the natural frequency. As the frequency is increased, the magnification factor converges toward unity for all damping ratios, i.e. the displacement amplitude approaches the nominal amplitude. The curves in Figure 2 and Figure 3 are called frequency response functions since they describe the response of a system to frequency-dependent dynamic input variable. Instead of magnification factor, they can be displayed for any other dynamic amplitude quantity, such as dynamic displacement, velocity, acceleration or force but are then not, by definition, frequency response functions. The displayed dynamic output is then herein simply denoted frequency response or response diagram.
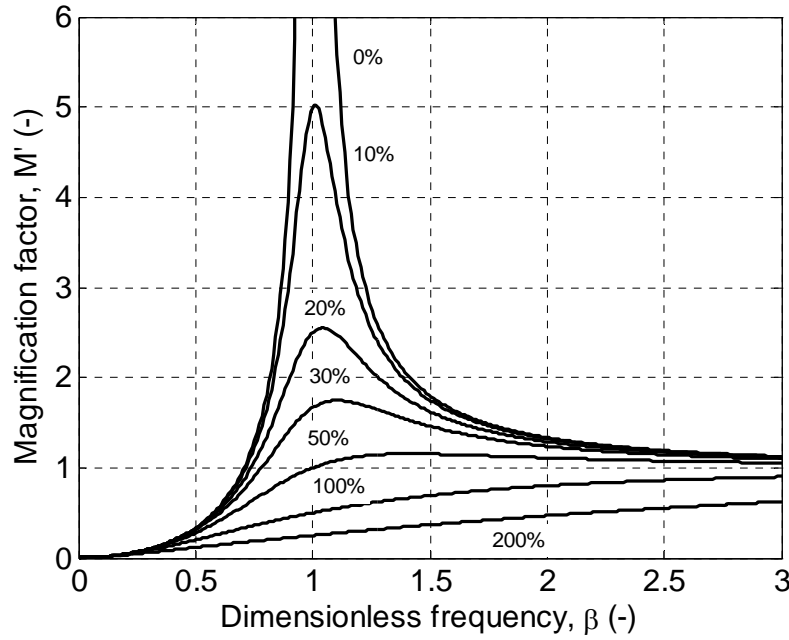
Figure 3. Dynamic magnification factor for rotating mass oscillators and different damping ratios.

2.2 Vertically Oscillating Foundations

The previous section described fundamental dynamic properties of SDOF systems. This section focuses on calculation of the dynamic response of a vertically oscillating foundation on an elastic half-space, as described by Lysmer & Richart (1966). For horizontal or rocking motion, see Hall (1967), and for torsion, see Richart et al. (1970). Gazetas (1983) presented equations for foundations on layered soil. Model tests have been conducted to experimentally determine the response of oscillating foundations under various conditions (e.g. Novak 1970; Baidya & Murali Krishna 2001; Mandal et al. 2012).

Lysmer & Richart (1966) showed how the behavior a vertically oscillating foundation on an elastic half-space can be simulated by a SDOF model, where spring stiffness and damping ratio are given by Equations 14 and 15.

$$k = \frac{4Gr_0}{1-\upsilon} \tag{14}$$

$$\zeta = \frac{0.425}{\sqrt{B_z}} \tag{15}$$

where G is soil shear modulus, r_0 is the footing radius, ν is Poisson's ratio of the soil and B_z is the mass ratio obtained by Equation 16.

$$B_z = \frac{1-\nu}{4} \frac{m}{\rho r_0^3} \tag{16}$$

where m is the total mass and ρ is the mass density of the soil. The total mass consists of two components. One is the mass of the foundation, m_0, including any external static load on it. The other part is called apparent mass, m_s, which corrects for the fact that stiffness decreases with frequency (Gazetas 1983). Different equations exist for calculating the apparent mass. In this study it becomes very small and is thus neglected. The total mass is given by Equation 17 and one expression for the apparent mass is given by Equation 18.

$$m = m_0 + m_s \tag{17}$$

$$m_s = \frac{1.08}{1-\nu}\rho r_0^3 \tag{18}$$

By applying the above equations to the SDOF model presented in the previous section, the dynamic behavior of a vertically oscillating foundation can be estimated. The main limitation with this and many other studies on the subject is the assumption that the subgrade is elastic. Since the stress-strain behavior of soil (especially non-plastic soil) is highly nonlinear, this simplification can lead to very large discrepancies between calculated and real dynamic responses. Soils with high plasticity, however, behave more elastic and the implications of treating the soil as perfectly linear are thus less severe. Nonlinear stress-strain behavior of soil, and a method to take these properties into account, is explained below.

2.3   Soil Nonlinearity

Deformation behavior of granular soil is often modeled by a hyperbolic stress-strain formulation (Kondner 1963a; Kondner 1963b; Hardin & Drnevic 1972a; Hardin & Drnevic 1972b). The hyperbolic shear stress τ is given by Equation 19.

$$\tau = \frac{G_{max}\gamma}{1 + \left|\frac{\gamma}{\gamma_r}\right|} \tag{19}$$

where G_{max} is the small-strain shear modulus, γ is the shear strain and γ_r is a reference strain. At very low strains the shear modulus is at its maximum, hence the denotation G_{max}. Equation 19 describes the so-called backbone curve (also called virgin curve or skeleton curve), which applies to virgin loading. When soil is subjected to cyclic loading, the stress-strain relationship forms a hysteresis loop often modeled by Masing Rule (Masing 1926), which implies magnifying the backbone curve by a factor of two during unloading and reloading. The backbone curve and hysteresis loop are shown in Figure 4.
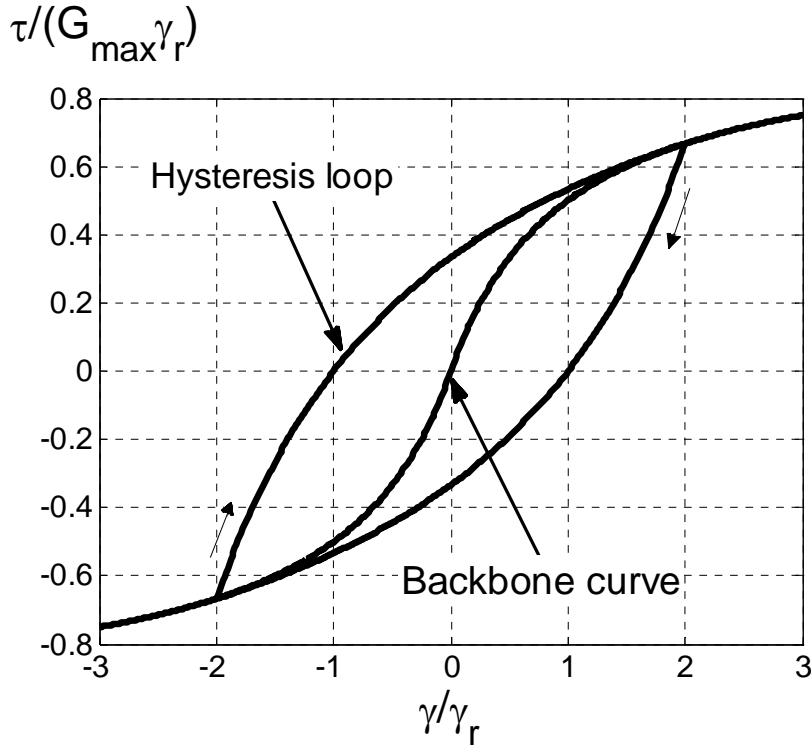
Figure 4. Normalized hyperbolic stress-strain relationship.

The small strain shear modulus can be estimated by Equation 20 according to Hardin (1978).

$$G_{max} = \frac{A \cdot OCR^k}{0.3 + 0.7e^2} P_a^{(1-n)} \sigma_0'^n \tag{20}$$

where A and n are a dimensionless parameters, OCR is the overconsolidation ratio, k is a parameter depending on plasticity index (PI), e is the void ratio, P_a is the atmospheric pressure (100 kPa) and $\sigma_0'^n$ is the effective isotropic confining pressure. Equation 20 is often seen with fixed values of A and n. However, these parameters vary with soil type and applying the equation with fixed values can thus be misleading. Studies investigating the values of the above parameters (e.g. Stokoe et al. 1999) have found A to vary in wide interval and n to vary slightly.

As can be seen in Figure 4, stiffness decreases with strain. Many authors have studied the strain-softening effect on the shear modulus (Seed et al. 1986; Vucetic & Dobry 1991; Rollins et al. 1998; Stokoe et al. 1999; Assimaki et al. 2000; Kausel & Assimaki 2002; Tatsuoka et al. 2003; Massarsch 2004; Zhang et al. 2005, among others). In the hyperbolic formulation described above, the shear modulus G decreases according to Equation 21.

$$\frac{G}{G_{max}} = \frac{1}{1 + \left|\frac{\gamma}{\gamma_r}\right|} \tag{21}$$

The reference strain is a curve-fitting parameter that depends on soil properties. It represents the strain at which the shear modulus has half the value of the small strain shear modulus. As shear strain increases, it affects not only the shear modulus, but also the damping ratio increases significantly. Hardin & Drnevic (1972b) proposed the formulation for damping ratio presented in Equation 22.

$$\frac{\zeta}{\zeta_{max}} = 1 - \frac{G}{G_{max}} \tag{22}$$

where ζ_{max} is the maximum damping ratio, which depends on the soil type and number of loading cycles N. Equation 23 shows the maximum damping ratio (in percent) for clean dry sand and Equation 24 presents the same parameter for saturated sand.

$$\zeta_{max} = 33 - 1.5\text{log}(N) \tag{23}$$

$$\zeta_{max} = 28 - 1.5\text{log}(N) \tag{24}$$

Rollins et al. proposed a model for shear modulus, Equation 25, and damping ratio, Equation 26, based on tests conducted on gravel.

$$\frac{G}{G_{max}} = \frac{1}{1.2 + 16|\gamma|(1 + 10^{-20|\gamma|})} \tag{25}$$

$$\zeta = 0.8 + 18(1 + 0.15|\gamma|^{-0.9})^{-0.75} \tag{26}$$

There is an apparent uncertainty in Rollins' equations. The shear modulus reduction ratio does not approach one for small strains due to the factor 1.2 in the denominator. As the ratio has to become unity for zero strain, the most obvious assumption is that this is a misprint in the paper.

A further formulation for shear modulus was proposed by Massarsch (2004), as presented in Equation 27.

$$\frac{G}{G_{max}} = \frac{1}{1 + \alpha|\gamma|(1 + 10^{-\beta|\gamma|})} \tag{27}$$

where α and β are empirical factors depending on PI. The variation of α and β are shown in Figure 5. The study was conducted with focus on fine-grained soils and thus no values are available for PI less than 10 %. However, Stokoe et al. (1999) found that strain-softening relationships of natural non-plastic soils and soils with low plasticity are very similar. The behavior of granular soil (non-plastic) can thus be estimated by applying values for PI = 10 %.
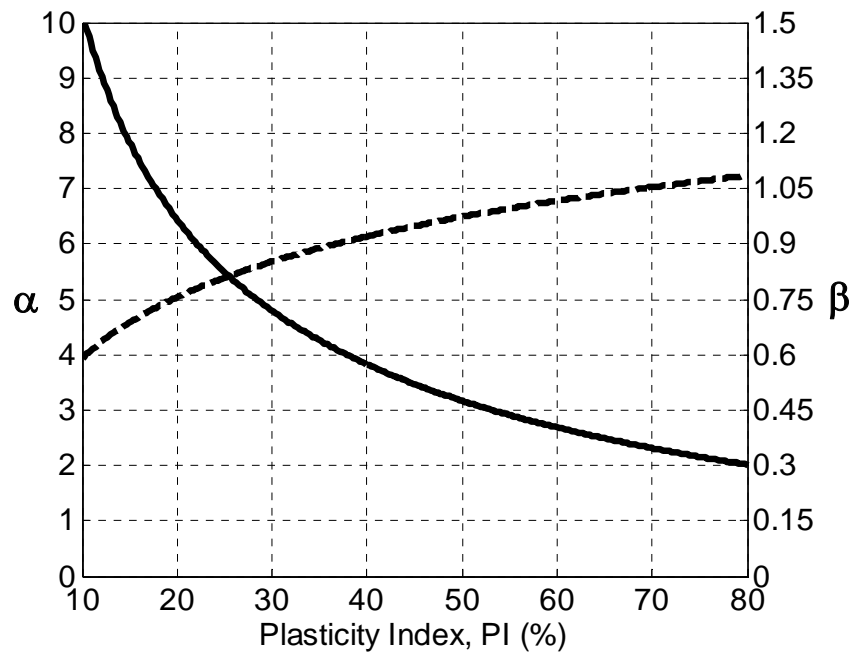
Figure 5. Variation of α and β with PI (after Massarsch 2004).

The shear modulus reduction ratios according to Equations 21, 25 and 27 are shown in Figure 6. A reference strain of 0.05 % was chosen, which is a typical value for sand (Stokoe et al. 1999). A modified version of Rollins' equation is also shown, where the term 1.2 has been replaced by 1.0. The reduction according to Massarsch is very similar to Hardin & Drnevic at low strains but implies slightly higher values of the shear modulus at large strains. The original expression by Rollins et al. is obviously not correct at small strains. The modified equation shows smaller shear modulus than the other expression at small and moderate strains, while larger at quite high strain level and similar to the other curves at very high strains.

Figure 7 shows the damping ratio calculated by Equation 26 (Rollins et al.), Equations 22 and 23 (Hardin & Drnevic, dry sand, first loading cycle) and Equations 22 and 24 (Hardin & Drnevic, saturated sand, first loading cycle). Seed et al. (1986) compiled results from many laboratory and field studies for strain-dependent damping ratio of sand. Equation 22 (using the reference strain 0.05 %, as above) is fitted to that data and shown in the same figure. The data from Seed et al. show a damping ratio close to that of clean saturated sand according to Hardin & Drnevic. For clean dry sand, the damping ratio is higher. The curve from Rollins et al. has a significantly lower damping ratio at high strains. All curves based on hyperbolic strain have one major disadvantage, namely that they approach zero for small strains. Since the damping ratio always is greater than zero, these models are unreliable at small strains.
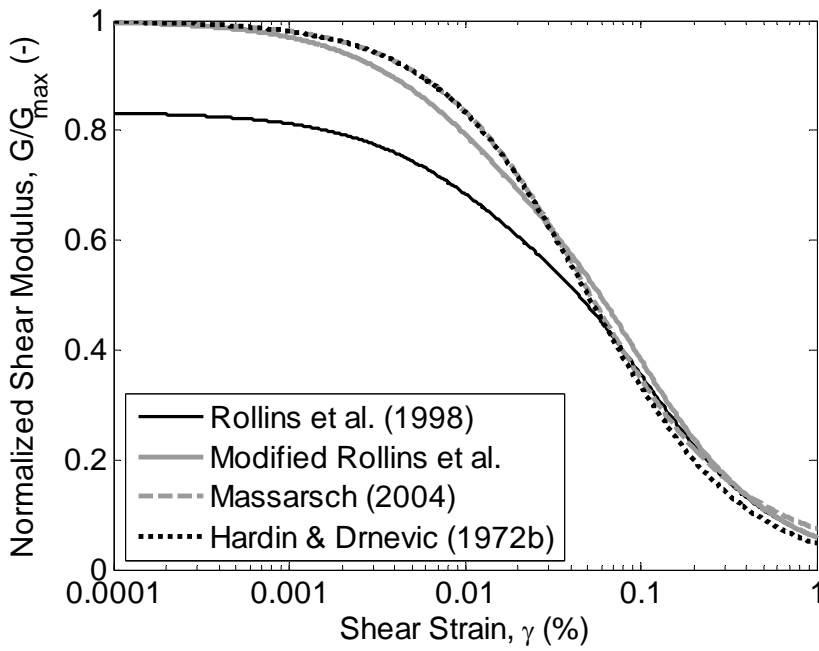
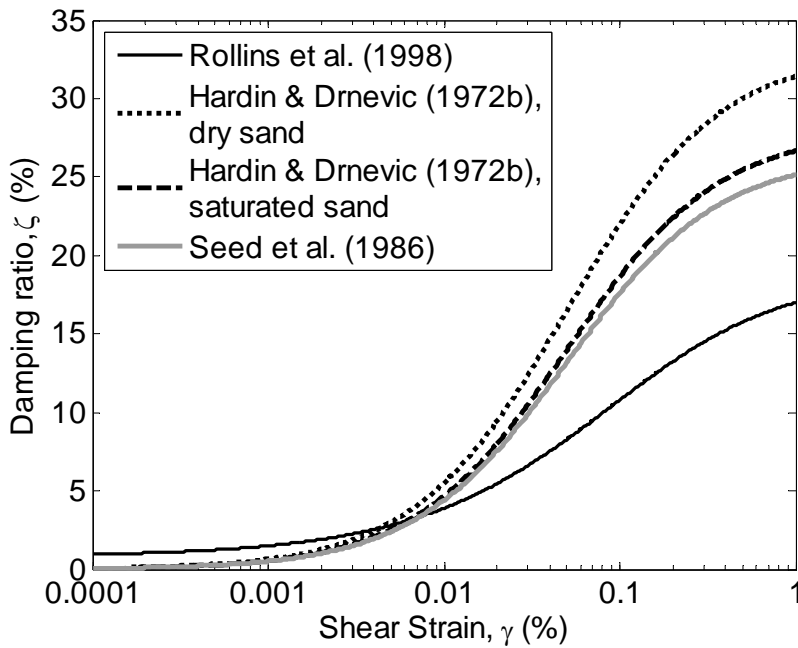*Figure 6. Strain-softening by different models.*

Figure 7. Comparison of damping ratio by different models.

2.4 Calculation of Foundation Response

The expressions given in Sections 2.1 and 2.2 can be used to calculate the frequency response for a vertically oscillating foundation on an elastic half-space. However, this is usually not sufficient for capturing the dynamic behavior of foundations on softening soil unless the strains are very small or the soil is highly plastic, as discussed above. During vibratory compaction, the case is normally the

opposite, i.e. very large strains and non-plastic soil. This section describes a simple method to incorporate strain-softening behavior into the calculation of frequency response, proposed by Wersäll et al. (2013). The procedure is explained in relation to the small-scale tests conducted with rotating mass oscillators described in Chapter 3 but is equally applicable to oscillations of other types of foundations under different dynamic load.

The first step is to determine the uncorrected displacement amplitude frequency response. This is done by first estimating the shear wave speed, c_S, and the mass density of the soil. The small-strain shear modulus can then be calculated by Equation 28.

$$G_{max} = \rho c_S^2 \tag{28}$$

Note that the shear wave speed in Equation 28 represents that at small strain and that it will decrease at larger strains. The small-strain shear wave speed can be measured by, for example, seismic tests. Alternatively, the small-strain shear modulus can be estimated directly by Equation 20. Determining Poisson's ratio of the soil and knowing the radius and mass of the foundation, the spring stiffness and damping ratio can be calculated by Equations 14-16. Depending on the relative size of the calculated apparent mass, it may be neglected and the mass of the foundation can be adopted as the total mass. Since the stiffness varies with frequency, each point on the curve will have a different natural frequency. The natural and dimensionless frequencies are calculated by Equations 6 and 7. Normally, the eccentric moment of the oscillator, $m_e e$, is known and the force amplitude can thus be calculated by Equation 10 for the frequency range of interest. The uncorrected frequency response for displacement amplitude is then obtained by Equation 8.

The next step is to calculate the shear strain in the soil. Each point in the response diagram represents a value of vertical displacement amplitude. This must first be converted to compressive strain and then to shear strain. Since a single value of strain is necessary for each frequency, strain must be assumed to be evenly distributed down to a certain depth. However, strain is not constant over depth but can rather be assumed to follow the Boussinesq distribution shown in Figure 8 (assuming the soil moduli are constant over depth). Figure 8 shows conceptually how the Boussinesq strain distribution can be approximated as triangular and then further simplified to a rectangular distribution.
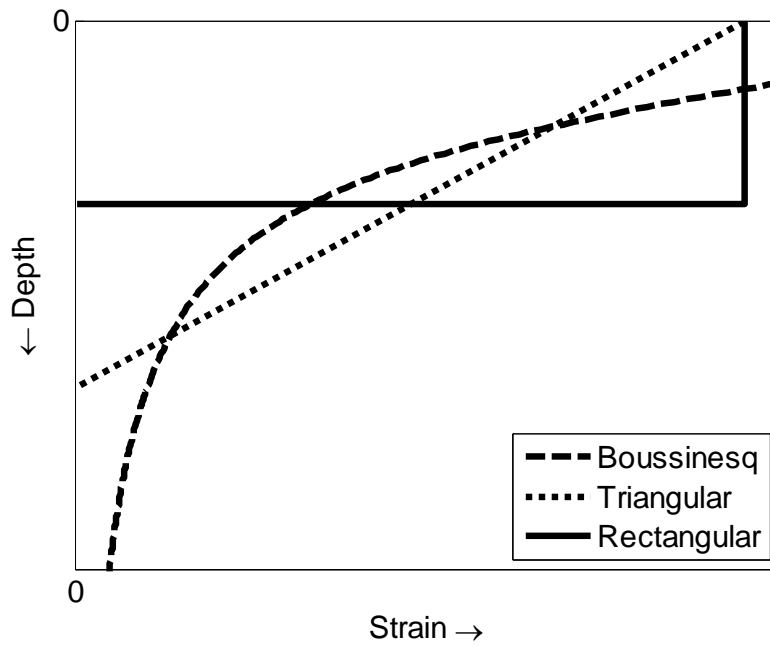
Figure 8. Simplification of Boussinesq strain to evenly distributed strain.

The depth to which the simplified rectangular strain distribution extends must thus be assumed, which gives the length of the strained element, L_ε. The compressive strain, ε, can then be calculated for each frequency by Equation 29 by using the displacement given by the response diagram.

$$\varepsilon = \frac{u_0}{L_\varepsilon} \tag{29}$$

By assuming axisymmetric conditions, the shear strain is calculated by Equation 30 (Atkinson & Bransby 1978).

$$\gamma = \frac{2}{3}\varepsilon(1 + v) \tag{30}$$

After the shear strain has been obtained, new strain-dependent values of the shear modulus and damping ratio can be calculated for every frequency by a suitable formulation. In this study, Equation 27 was applied for shear modulus and Equation 22 for damping ratio. The maximum damping ratio was assumed to be 33 %, based on Equation 23.

The new shear modulus and damping ratio are then used, applying the same procedure, to calculate the frequency response for displacement, compressive strain and shear strain. The new shear strain again yields new values of the shear modulus and damping ratio and the process is repeated. This is iterated until the response diagrams converge with sufficiently small variations between iterations, for each value of frequency. The final displacement function then gives the frequency response for velocity amplitude v_0, acceleration amplitude a_0 and force amplitude by Equations 31 to 33.

$$v_0 = \omega u_0 \tag{31}$$

$$a_0 = \omega^2 u_0 \tag{32}$$

$$F_0 = k u_0 \tag{33}$$

3   DESCRIPTION OF SMALL-SCALE TESTS

Small-scale compaction tests were conducted in laboratory environment. The tests were divided over two main setups and several test series. An electro-dynamic oscillator was used in the first setup, creating high controllability. The second setup utilized rotating mass oscillators with less controllability but higher resemblance to field conditions. Both setups were purpose-built for the tests. Since the tests are described in detail in the appended papers, this chapter provides only a summary of the test setups and results.

Sand was placed in a box having inner measurements 1100 mm x 700 mm x 370 mm (width x length x height). The boundaries were coated with 30 mm of expanded polystyrene to reduce vibration reflections and the bottom of the box consisted of the concrete floor below the box. The filling method is crucial to obtain similar test conditions as it has a strong influence on the initial density of the sand (Rad & Tumay 1987). Due to the large number of tests and the large sand volume, the material was filled by pouring. Since there was no target density but rather a similar density in all tests that was important, this method was considered sufficient. Other more precise methods, such as raining, would be unrealistically time-consuming. The pouring was performed in the same way by the same person to minimize any differences in initial density.

3.1   Tests with Electro-Dynamic Oscillator

This type of oscillator consists of a static mass and a significantly smaller oscillating mass on top. In the first setup, shown in Figure 9, the static mass was connected to a steel rod with a circular steel plate, 84 mm in diameter, at the other end. The rod was running through two low-friction polytetrafluoroethylene (Teflon) rings, allowing the rod to move only in the vertical direction. The plate was placed directly on the sand surface. The advantage with an electro-dynamic oscillator is that dynamic quantities can be adjusted in real-time, thus making the tests very controllable. The system can be illustrated as a coupled mass-spring-dashpot model, shown in Figure 10. The dynamic force $F(t)$ is generated in the spring between the oscillating and static masses. Since the oscillating mass is much smaller than the static mass, the soil response does not influence its vibrations, which means that measurements on the oscillating mass are independent of soil-compactor resonances. This provides the opportunity to conduct tests under constant dynamic load. The total mass of the vertically moving system was 37.4 kg.

One accelerometer was placed on the oscillating mass and one on the static mass. A force transducer was placed between the plate and the rod measuring the reaction force. Furthermore, the rod was connected to a linear variable differential transformer (LVDT), measuring the vertical settlement of the plate. Acceleration signals from the accelerometers were integrated in the amplifiers so that particle velocity was recorded. An external amplifier controlled the amplitude of the oscillator and the frequency was adjusted by a function generator. Geophones were placed in the sand, on the box perimeter and on the concrete floor. A vertical accelerometer was buried in the sand, 20 cm below the plate.
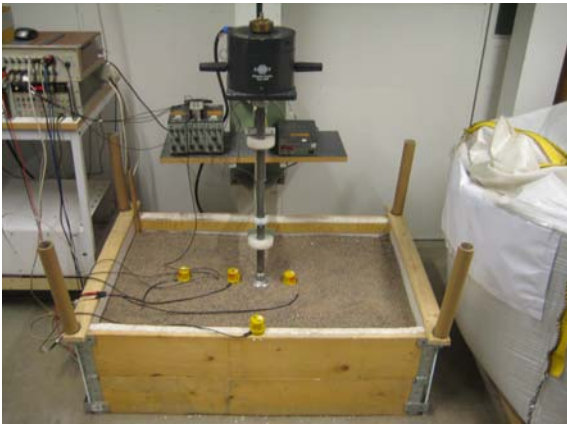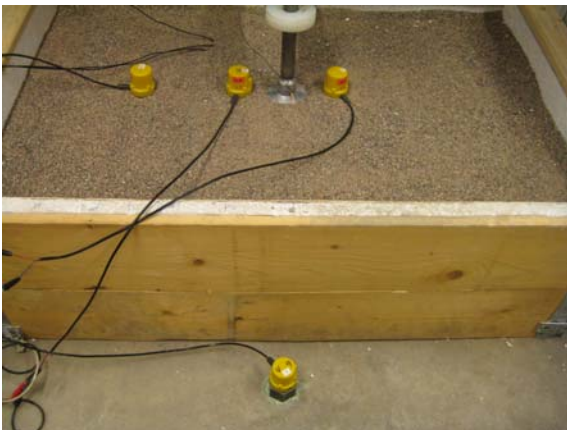
(a)

(b)

(c)

(d)

(e)

(f)

Figure 9. Tests with electro-dynamic oscillator. (a) Preparation of test box. (b) Preloading. (c) The complete test setup. (d) Settlement and heave after compaction. (e) Measurement with geophones inside and outside of the test box. (f) Test for investigation of soil displacement.
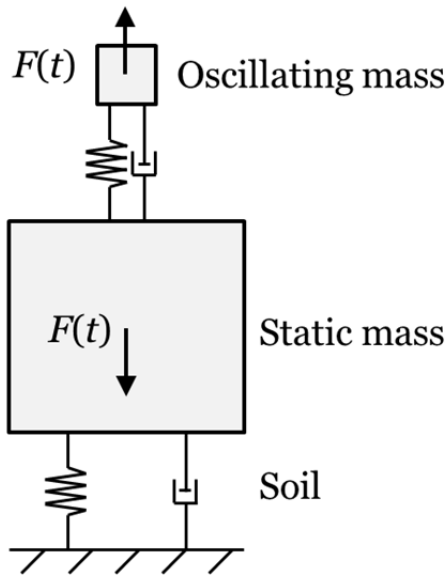
Figure 10. Representation of tests with the electro-dynamic oscillator as a coupled mass-spring-dashpot system.

Each test was conducted with frequency sweep and a constant particle velocity on the moving mass. The frequency was controlled by the function generator and the velocity amplitude was adjusted manually on the oscillator amplifier. The measured acceleration signal was integrated and plotted on a computer screen in real-time for adjusting the amplitude. The tests are described thoroughly in Wersäll and Larsson (2013).

3.2 Tests with Rotating Mass Oscillators

To obtain conditions that are more similar to those during roller compaction, a new compactor was manufactured using two rotating mass oscillators together giving rise only to a vertical component. Except for the new type of oscillators, the equipment, shown in Figure 11, was very similar as in the previous small-scale tests. A mass-spring-dashpot representation would here only include one mass where the force is directly applied. An accelerometer was mounted on the bottom plate and a force transducer was placed between the plate and the rod. In the same manner as the previous tests, the vertical settlement was measured by an LVDT. In some tests, geophones were placed in the sand and on the box perimeter or outside the box. The mass of the vertically moving system was 28.8 kg.

The tests, described in Wersäll et al. (2013), were conducted at discrete frequencies, i.e. not using frequency sweep as in the previous tests. The sand was replaced between each test. When using rotating mass oscillators, the eccentric moment is constant and the applied force increases with the square of frequency. It was thus not possible to control particle velocity or any other dynamic quantity. This is true also for compaction with vibratory roller. In each test, the sand was compacted for 30 seconds and the settlement was recorded.

(a)

(b)

(c)

(d)

(e)

(f)

Figure 11. Tests with rotating mass oscillators. (a) Test setup. (b) Oscillators with protective caps removed. (c) Preloading by vibrating a wooden plate. (d) After completion of a test on dry sand. (e) After completion of a test on wet sand. (f) Imprint in wet sand after test and removal of the plate.

3.3   Results of Small-Scale Tests

In the tests using the electro-dynamic oscillator, compaction was significantly enhanced close to the resonant frequency with hardly any compaction sufficiently below or above this frequency. The tests with rotating mass oscillators, on the other hand, showed a more complex relationship between frequency and compaction. The applied force increased with frequency, producing a very high degree of compaction at the higher frequencies and hardly any compaction at the low frequencies. In the mid-range, however, there was a resonant amplification, which was quite modest compared to the amplification in the previous tests. The main differences between the two test setups were the following:

- The dynamic load in comparison with the static weight.

- The variation of input load with frequency – constant particle velocity in the first test setup and force increasing with the square of frequency in the second setup.

- Higher dynamic loads in the second setup.

The difference in resonant amplification originates from the differences between tests, as listed above. Since the dynamic-to-static load ratios are significantly lower than one and far above one, respectively, the fundamental dynamic behavior is essentially different. Furthermore, since force is increasing drastically with frequency during operation of the rotating mass oscillators, resonant amplification becomes less pronounced. The most influential aspect, however, is most likely the high dynamic load, giving rise to large strains, which produces a significant reduction in the soil stiffness while the damping ratio increases, as has been explained in Section 2.3. This causes the curve to flatten out (Wersäll et al. 2013). The effect of increased damping ratio can be understood by observing Figure 3. In spite of the modest amplification at resonance, it is probable that this effect can be utilized in compaction by vibratory roller, as has been discussed in Paper II.

Frequency response of dynamic quantities was calculated by the equivalent linear calculation procedure described in Chapter 2. When parameters of the rotating mass oscillator tests were applied to the equations, the results matched measured data well. The conclusion is thus drawn that this method accurately can predict the dynamic behavior of oscillating foundations during compaction or other applications where large strains are involved.

4   SUMMARY OF APPENDED PAPERS

4.1   Paper I

Small-Scale Testing of Frequency-Dependent Compaction of Sand Using a Vertically Vibrating Plate

Carl Wersäll and Stefan Larsson

Published in ASTM Geotechnical Testing Journal 2013:36(3)

The paper presents results from 85 small-scale tests that were conducted using a vertical electro-dynamic oscillator, connected to a plate and placed on a sand bed. Frequency was adjusted continuously to assess its influence on compaction of the underlying sand. The results showed that the rate of compaction with this type of compactor is significantly magnified at, and close to, the resonant frequency. The results indicated that velocity amplitude is a crucial quantity in obtaining sufficient compaction in for the test setup used. While a large velocity amplitude gave rise to a large degree of compaction, it also caused significant soil displacement and heave. Tests showed that compaction is closely related to strain-softening since the strain above which moduli start to decrease coincides with the strain required for compaction of the soil.

4.2   Paper II

Frequency Variable Surface Compaction of Sand Using Rotating Mass Oscillators

Carl Wersäll, Stefan Larsson, Nils Rydén and Ingmar Nordfelt

Submitted to ASTM Geotechnical Testing Journal in November 2013

The objective of this paper is to study the influence of frequency in compaction tests using rotating mass oscillators. Results from 105 small-scale tests, conducted using a vertically oscillating plate, are presented. The soil underlying the plate was dry sand, or sand close to the optimum water content. The results showed that there is a resonant amplification, providing slightly higher degree of compaction. Most effective compaction is obtained at very high frequencies. The paper discusses the implications for roller compaction and suggests that a slightly lower frequency may prove more efficient. An iterative method for calculating dynamic response of the plate, incorporating strain-dependent properties of the soil, is also presented. The calculated frequency response agrees well with measured quantities.

SUMMARY OF APPENDED PAPERS

5   CONCLUSIONS AND FURTHER RESEARCH

This thesis presents results from small-scale tests using a vertically oscillating plate. Two test setups were manufactured, the first using an electro-dynamic oscillator and the second utilizing two rotating mass oscillators. The frequency response was calculated by combining theory for vibrating foundations on elastic half-space with an iterative procedure for estimating strain-dependent properties of soil. The main conclusions of all studies incorporated in this thesis are listed below:

- Soil compaction by a vibratory plate is frequency-dependent, providing an amplified degree of compaction close to the resonant frequency.
- The resonant amplification is more modest during compaction using a high dynamic force, mainly due to large strain causing high damping and strain-softening.
- The small-scale tests using an electro-dynamic oscillator gave quite a large amount of soil displacement and heave while these were small in the rotating mass oscillator tests.
- No dynamic quantity is solely governing for the degree of compaction.
- The water content of the soil has no apparent effect on the dynamic behavior of the vibrating plate or on the frequency dependence of compaction. It does, however, have positive effect on the degree of compaction.
- Compaction is closely related to strain-softening. The strain level, above which the stiffness of the soil starts to decrease, coincides with the strain required to obtain rearrangement of soil particles.
- The proposed method to calculate frequency response captures well the measured dynamic behavior the second small-scale test.

The settlement velocities in all tests using the electro-dynamic oscillator are shown in Figure 12. A higher velocity implies a higher rate of compaction. The total settlement in the tests using the rotating mass oscillators is shown in Figure 13. The figures illustrate the frequency dependence of compaction using the different equipment.

The results above are valuable for a fundamental understanding of soil compaction and also for the dynamics of oscillating foundations. To develop this further and to make it practically applicable to compaction using vibratory roller, the following proposals for further research are suggested:

- Investigate the influence of changing the eccentricity, i.e. the dynamic force, in rotating mass oscillator tests.
- Investigate the influence of sand layer thickness and stiffness of the subsoil.
- Compare calculated frequency response to small-scale tests with electro-dynamic oscillator and to other practical applications.
- Do extensive full-scale tests with vibratory roller, compacting granular soil at discrete frequencies, but in a wide frequency span.
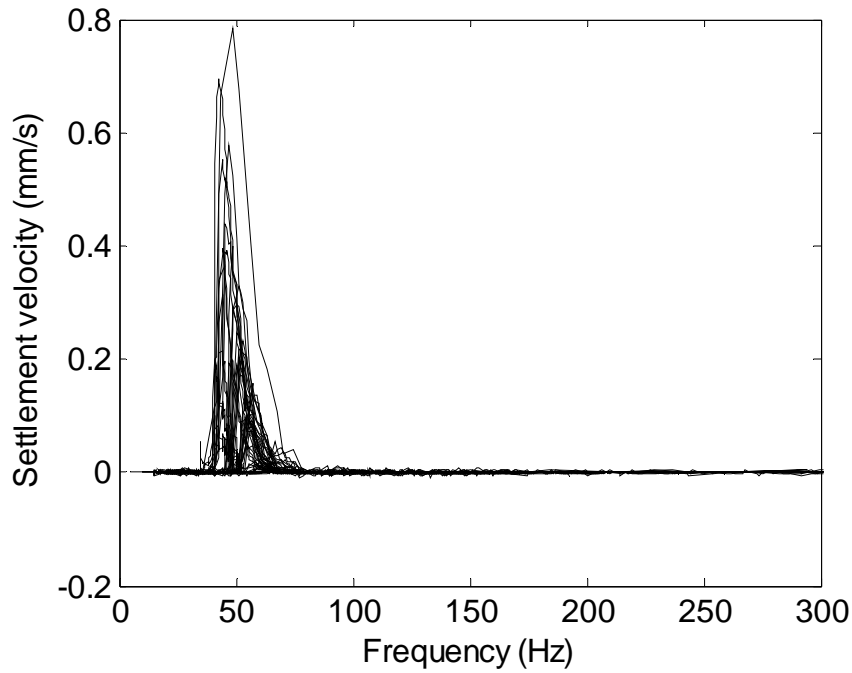- Simulate the small-scale tests and roller compaction by distinct element modeling.

Figure 12. Displacement velocity in tests using electro-dynamic oscillator. Modified after Wersäll and Larsson (2013).
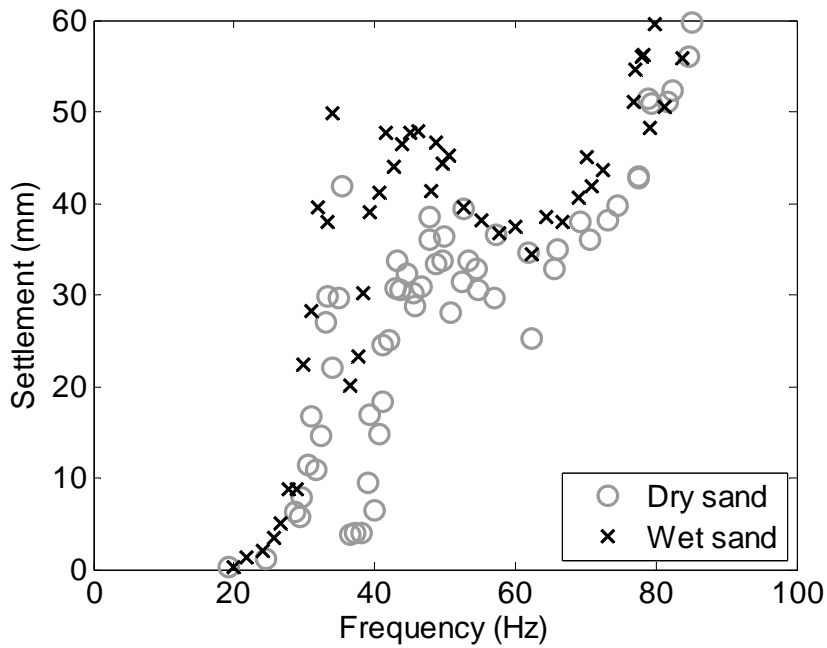

Figure 13. Total settlement in tests using rotating mass oscillators. From Wersäll et al. (2013).

REFERENCES

Adam, D., 1996., *Flächendeckende Dynamische Verdichtungskontrolle (FDVK) mit Vibrationswalzen* [Continuous Compaction Control with Vibratory Rollers], PhD thesis, University of Vienna, Vienna, Austria, 267 p., (in German).

Anderegg, R. and Kaufmann, K., 2004, "Intelligent Compaction with Vibratory Rollers," *Transportation Research Record. 1868*, Transportation Research Board, Washington, D.C., pp. 124–134.

Assimaki, D., Kausel, E., and Whittle, A., 2000, "Model for Dynamic Shear Modulus and Damping for Granular Soils." *Journal of Geotechnical and Geoenvironmental Engineering*, Vol. 126, No. 10, pp. 859–869.

Atkinson, J. H., Bransby, P. L., 1978, *The Mechanics of Soils: An Introduction to Critical State Soil Mechanics*, McGraw-Hill, London, 375 p.

Baidya, D. K. and Murali Krishna, G., 2001, "Investigation of Resonant Frequency and Amplitude of Vibrating Footing Resting on a Layered Soil System," *Geotechnical Testing Journal*, Vol. 24, No. 4, pp. 409–417.

Bernhard, R. K., 1952, "Static and Dynamic Soil Compaction," *Highway Research Board Proceedings*, Vol. 31, pp. 563–592.

Converse, F. J., 1953, "Compaction of Sand at Resonant Frequency," *ASTM Special Technical Publication*, No. 156, pp. 124–137.

D'Appolonia, D. J., Whitman, R. V. and D'Appolonia, E., 1969, "Sand Compaction with Vibratory Rollers," *Journal of the Soil Mechanics and Foundations Division*, Vol. 95, No. 1, pp. 263–284.

Dobry, R. and Whitman, R. V., 1973, "Compaction of Sand on a Vertically Vibrating Table," *Evaluation of Relative Density and Its Role in Geotechnical Projects Involving Cohesionless Soils*, ASTM Special Technical Publication, No. 523, pp. 156–170.

Facas, N. W., Rinehart, R. V. and Mooney, M. A., 2011, "Development and Evaluation of Relative Compaction Specifications Using Roller-Based Measurements," *Geotechnical Testing Journal*, Vol. 34, No. 6, pp. 634–642.

Forssblad, L., 1965, "Investigations of Soil Compaction by Vibration," *Acta Polytechnica Scandinavica*, No. 34.

Forssblad, L., 1980, "Compaction Meter on Vibrating Rollers for Improved Compaction Control," *Proceedings of International Conference on Compaction*, Vol. 2, Paris, France, pp. 541–546.

Forssblad, L., 1981, *Vibratory Soil and Rock Fill Compaction*, Dynapac Maskin AB, Stockholm, Sweden, 175p.

Gazetas G., 1983, "Analysis of Machine Foundation Vibrations: State-of-the-Art," *International Journal of Soil Dynamics and Earthquake Engineering*, Vol. 2, No. 1, pp. 2-43.

Hall, J. R., Jr., 1967, "Coupled Rocking and Sliding Oscillations of Rigid Circular Footings," *Proceedings of the International Symposium on Wave Propagation and Dynamic Properties of Earth Materials*, Albuquerque, New Mexico, pp. 139-148.

Hardin, B. O., 1978, "The Nature of Stress-Strain Behavior of Soils," *Proceedings of the ASCE Geotechnical Engineering Division Specialty Conference on Earthquake Engineering*, Vol. 1, Pasadena, California, pp. 3-90.

Hardin, B. O. and Drnevich, V. P., 1972a, "Shear Modulus and Damping in Soils: Design Equations and Curves," *Journal of the Soil Mechanics and Foundations Division*, Vol. 98, No. 7, pp. 667–692.

Hardin, B. O. and Drnevich, V. P., 1972b, "Shear Modulus and Damping in Soils: Measurement and Parameter Effects," *Journal of the Soil Mechanics and Foundations Division*, Vol. 98, No. 6, pp. 603-624.

Hertwig, A., 1936, "Means for Consolidating the Ground," US Patent 2039078.

Johnson, A. W. and Sallberg, J. R., 1960, *Factors that Influence Field Compaction of Soils*, Highway Research Board, Bulletin No. 272, 206 p.

Kausel, E. and Assimaki, D., 2002, "Seismic Simulation of Inelastic Soils via Frequency-Dependent Moduli and Damping." *Journal of Engineering Mechanics*, Vol. 128, No. 1, pp. 34–47.

Kondner, R. L., 1963a, *A Hyperbolic Stress-strain Formulation for Sands*, Northwestern University, 60 p.

Kondner, R. L., 1963b, "A Hyperbolic Stress-Strain Response: Cohesive Soils," *Journal of the Soil Mechanics and Foundations Division*, Vol. 89, No. 1, pp. 115-143.

Lorenz, H., 1960, *Grundbau-Dynamik* [Foundation Dynamics], Springer-Verlag, Berlin, 308 p., (in German).

Lysmer, J. and Richart, F. E., Jr., 1966, "Dynamic Response of Footings to Vertical Loading," *Journal of the Soil Mechanics and Foundations Division*, Vol. 92, No. 1, pp. 65–91.

Mandal, A., Baidya, D. K. and Roy, D., 2012, "Dynamic Response of the Foundations Resting on a Two-layered Soil Underlain by a Rigid Layer," *Journal of Geotechnical and Geological Engineering*, Vol. 30, No. 4, pp. 775-786.

Masing, G., 1926, "Eigenspannungen und Verfestigung beim Messing," *Proceedings of the second International, Congress on Applied Mechanics*, pp. 332-335, (in German).

Massarsch, K. R., 2004, "Deformation Properties of Fine-Grained Soils from Seismic Tests," Keynote lecture, *Proceedings of the Second International Conference on Site Characterization, ISC'2*, Porto, Portugal, pp. 133–146.

Mooney, M. A. and Rinehart, R. V., 2009, "In Situ Soil Response to Vibratory Loading and Its Relationship to Roller-Measured Soil Stiffness," *Journal of Geotechnical and Geological Engineering*, Vol. 135, No. 8, pp. 1022–1031.

Novak, M., 1970, "Prediction of Footing Vibrations," *Journal of the Soil Mechanics and Foundations Division*, Vol. 96, No. 3, pp. 837-861.

Rad, N. S. and Tumay, M. T., 1987, "Factors Affecting Sand Specimen Preparation by Raining," *Geotechnical Testing Journal*, Vol. 10, No. 1, pp. 31–37.

Richart, F. E., Jr., Hall, J. R., Jr. and Woods, R. D., 1970, *Vibrations of soils and foundations*, Prentice-Hall, Englewood Cliffs, New Jersey, 414 p.

Rollins, K. M., Evans, M. D., Diehl, N. B. and Daily, W. D. III, 1998, "Shear Modulus and Damping Relationships for Gravels." *Journal of Geotechnical and Geoenvironmental Engineering*, Vol. 124, No. 5, pp. 396–405.

Schnabel, P. B., Lysmer, J. and Seed, H. B., 1972, *SHAKE: a Computer Program for Earthquake Response Analysis of Horizontally Layered Sites*, Earthquake Engineering Research Center, University of California, Berkeley, 92 p.

Seed, H. B., Wong, R. T., Idriss, I. M. and Tokimatsu, K., 1986, "Moduli and Damping Factors for Dynamic Analyses of Cohesionless Soils," *Journal of Geotechnical Engineering*, Vol. 112, No. 11, pp. 1016–1032.

Stokoe, K. H., II, Darendeli, M. B., Andrus, R. D., and Brown, L. T., 1999, "Dynamic soil properties: Laboratory, field and correlation Studies," *Proceedings of the Second International Conference on Earthquake Geotechnical Engineering*, Vol. 3, Lisbon, Portugal, pp. 811–845.

Susante, P. J. and Mooney, M. A., 2008, "Capturing Nonlinear Vibratory Roller Compactor Behavior through Lumped Parameter Modeling," *Journal of Engineering Mechanics*, Vol. 134, No. 8, pp. 684-693.

Tatsuoka, F., Masuda, T., Siddiquee, M., and Koseki, J., 2003, "Modeling the Stress-Strain Relations of Sand in Cyclic Plane Strain Loading." *Journal of Geotechnical and Geoenvironmental Engineering*, Vol. 129, No. 5, pp. 450–467.

Thurner, H. and Sandström, Å., 1980, "A New Device for Instant Compaction Control," *Proceedings of International Conference on Compaction*, Vol. 2, Paris, France, pp. 611–614.

Tschebotarioff, G. P. and McAlpin, G. W., 1947, *Effect of Vibratory and Slow Repetitional Forces on the Bearing Properties of Soils*, Civil Aeronautics Administration, Technical Development Report No. 57, 70 p.

Vucetic, M. and Dobry, R., 1991, "Effect of Soil Plasticity on Cyclic Response," *Journal of Geotechnical Engineering*, Vol. 117, No. 1, pp. 89–107.

Wersäll, C. and Larsson, S., 2013, "Small-Scale Testing of Frequency-Dependent Compaction of Sand Using a Vertically Vibrating Plate," *Geotechnical Testing Journal*, Vol. 36, No. 3, pp. 1-10.

Wersäll, C., Larsson, S., Rydén, N. and Nordfelt, I., 2013, Frequency Variable Surface Compaction of Sand Using Rotating Mass Oscillators, Submitted to Geotechnical Testing Journal.

Yoo, T-S. and Selig, E. T., 1979, "Dynamics of Vibratory-Roller Compaction," *Journal of the Geotechnical Engineering Division*, Vol. 105, No. 10, pp. 1211–1231.

Zhang, J., Andrus, R., and Juang, C., 2005, "Normalized Shear Modulus and Material Damping Ratio Relationships." *Journal of Geotechnical and Geoenvironmental Engineering*, Vol. 131, No. 4, pp. 453–464.

Paper I

Small-Scale Testing of Frequency-Dependent Compaction of Sand Using a Vertically Vibrating Plate

Wersäll, C. and Larsson, S.

Carl Wersäll[1] and Stefan Larsson[1]

Small-Scale Testing of Frequency-Dependent Compaction of Sand Using a Vertically Vibrating Plate

ABSTRACT: Vibratory rollers generally operate at a fixed vibration frequency. It is hypothesized that the compaction of soil could be made more efficient if the frequency could be adapted to specific project conditions. In order to study the applicability to surface compaction, the frequency dependence of compacting dry sand with a vertically vibrating plate was investigated experimentally in 85 small-scale tests. Tests were performed in a test box simulating the free-field condition and with concrete underlying the sand bed. The results show that there is a distinct frequency dependence, implying a significantly improved compaction effect close to the compactor–soil resonant frequency. It is suggested that particle velocity is the governing amplitude parameter for vibratory soil compaction, rather than displacement or acceleration. As the soil is compacted, it is also displaced, resulting in surface heave. A larger vibration amplitude implies greater displacement relative to the compacted volume. It was also observed that the compaction and strain-dependent reduction of soil stiffness are closely related.

KEYWORDS: compaction, resonant frequency, strain softening, vibration, particle velocity

Introduction

The use of vibratory rollers as compaction equipment for embankments and landfills has been well established for many decades. Roller manufacturers have recently struggled with stricter environmental regulations necessitating the use of more fuel-efficient, low-emission diesel engines. Machines have also increased in size, improving their compaction efficiency. Furthermore, control systems, safety issues, and the driver's working environment have been topics for research and development. However, little effort has been made since the 1970s to improve the compaction effect by reevaluating and investigating fundamental compaction parameters. One such parameter is the operating frequency f of the vibrator. Since the 1970s, the main research topic has been continuous compaction control (CCC) using vibration measurements from sensors on the roller (e.g., Forssblad 1980; Thurner and Sandström 1980; Adam 1996; Anderegg and Kaufmann 2004; Mooney and Rinehart 2009; Rinehart and Mooney 2009; Facas et al. 2011). The analysis approach for evaluating measured vibrations in CCC is based on the lumped-parameter model suggested by Yoo and Selig (1979). This model consists of two coupled mass-spring-dashpot systems. In recent years, finite element models simulating the compaction process have been developed. Topics studied numerically include the prediction of compacted density (Lee and Gu 2004; Xia 2012) and the

comparison of compaction methods (Arnold and Herle 2009). However, no one has investigated the influence of f on the compacted density. Full-scale testing has been performed by manufacturers, optimizing parameters such as the layer thickness, number of passes, and static weight of the roller. However, these studies have generally been performed for commercial purposes and remain unpublished.

In the early years of soil compaction research, optimal compaction frequency was intensively discussed. Some authors argued that compaction was most effectively carried out at the compactor–soil resonant frequency f_r (Johnson and Sallberg 1960), whereas others argued that f is not of great importance (Forssblad 1965). However, many of these statements were mere speculation, partly because of the lack of frequency-variable compaction equipment and advanced measurement techniques at the time. Bernhard (1952) performed laboratory tests, concluding that compaction is more efficient at f_r. The same was observed by Converse (1954) in extensive field tests using a plate-mounted vertical vibrator compacting sand in a test pit. It has long been known that vibrating plates are more efficient than rollers in compacting soil (Lewis 1961). However, they are not practical for use over large areas, in contrast to rollers. Dobry and Whitman (1973) performed compaction tests on sand in a mold on a vibrating table and found that f was important for compaction in certain acceleration intervals. Naturally, threshold values of the amplitude of acceleration a_0, velocity v_0, or displacement u_0 must be exceeded in order for satisfactory compaction to be obtained. Several studies have shown that compaction is most efficient when a_0 exceeds $1\,g$ (D'Appolonia et al. 1969; Dobry and Whitman 1973). The above results have not been shown for roller compaction, and the optimal f of rollers remains to be investigated.

A review of existing literature shows that very few have investigated roller compaction experimentally and that no one has, to the authors' knowledge, studied the frequency dependence of roller compaction. The objective of this paper is to study fundamental frequency-dependent properties of granular soil. The purpose is to present the results of some recent small-scale tests in which dry sand was compacted using a vertically vibrating plate. It is hypothesized that the f_r of the compactor–soil system can be utilized to obtain a higher degree of compaction in a shorter time period, as opposed to frequencies below or above resonance. The relationship between strain softening and the magnitude of compaction is also investigated. Other authors have performed similar vibration tests with varying values of f (Baidya and Murali Krishna 2001; Nagappagowda and Thulasiram in press). However, the relation between f and the compaction effect has not been investigated experimentally. The scale of the tests is justified because the size of the vibrating plate needs to be sufficiently large in relation to the soil grains and the test box needs to be as large as possible, with the scale small enough to allow control over and repeatability of laboratory conditions.

The test results presented in this paper cannot be directly applied to roller compaction. The influence of the ratio of dynamic force and static weight must be considered. In the present tests, the static weight is larger than the dynamic force, whereas the opposite is true for compaction by roller. Furthermore, the influence of a moving load with a different contact area needs to be investigated. These are topics for further studies. However, this paper contains unique results regarding the compaction of sand that provide an opportunity to study these concepts in relation to roller compaction. The findings are also applicable to other granular materials and settlement in soil due to other types of vibratory loading.

Methods and Experimental Setup

The influence of f on the compaction effect was investigated in small-scale tests in a sand-filled box using a vertical electrical vibration exciter. The test equipment and setup are shown in Fig. 1. The box consisted of a wooden frame bolted directly to the concrete floor. The inside of the vertical boundaries was coated with 30 mm of expanded polystyrene to reduce wave reflections. The inner
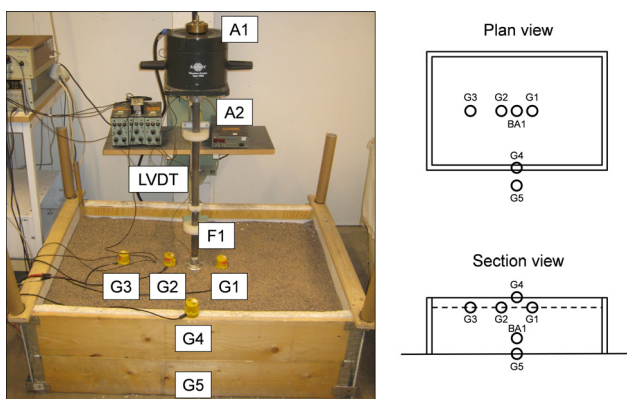

FIG. 1—*Test box and experimental setup. The dashed line in the section view indicates the sand surface.*

measurements of the box were $1100 \, \text{mm} \times 700 \, \text{mm} \times 370 \, \text{mm}$ ($W \times L \times H$). The ratios of the inner width/plate diameter and inner length/plate diameter were 8.1 and 13.1, respectively. The size of the box was considered sufficiently large for the boundaries not to affect the compaction frequency dependence of the plate. Baidya and Murali Krishna (2001) found that the resonant amplitude, but not f_r, was affected by the size of the test box in similar tests.

Selection of Test Parameters

In order to investigate the influence of f, the compaction efficiency must be compared at different values of f at a selected constant amplitude. A frequent subject of discussion is what the governing vibration amplitude parameter is for soil compaction—u_0, v_0, or a_0. In this study, the hypothesis is that, except for f, v_0 controls the degree of compaction. One reason is that the shear strain γ is proportional to the particle velocity v and is crucial for obtaining a rearrangement of particles. Another reason is that the power P (energy per unit time) of vibrations that propagate into the soil from a dynamic exciter placed on the soil surface is proportional to v_0^2. This is shown briefly below (for a detailed explanation, see Wersäll et al. 2012). Displacement of the vibrator u can be expressed by Eq 1.

$$u = u_0 \cos(\omega t) \tag{1}$$

in which ω is the circular frequency. If we consider the vibrating mass on the soil as a mass-spring-dashpot system, the input force can be divided into the spring force F_k and the dashpot force F_c, given by Eqs 2 and 3, respectively.

$$F_k = ku = ku_0 \cos(\omega t) \tag{2}$$

$$F_c = c\frac{du}{dt} = -\omega c u_0 \sin(\omega t) \tag{3}$$

where:
  $k =$ spring stiffness, and
  $c =$ damping coefficient.

Because the spring consumes no energy, all energy consumption takes place in the dashpot, and the damped energy is equal to the energy that is manifested as propagating waves. Plotting F_c versus u results in an elliptical path. The area of the ellipse gives the energy consumed in one cycle, expressed by Eq 4.

$$W_c = \pi \omega c u_0^2 \tag{4}$$

With the application of $\omega = 2\pi f$ and $v_0 = \omega u_0$, the vibration power consumed by the dashpot, and thus propagating into the soil, can be calculated using Eq 5.

$$P = f W_c = \frac{1}{2} c(\omega u_0)^2 = \frac{1}{2} c v_0^2 \tag{5}$$

It is concluded from Eq 5 that P is proportional to v_0^2, and thus a constant value of v_0 results in a constant vibration energy per unit time. Other dynamic parameters, such as the spans of f and v_0, were selected based on initial tests and limitations of the test equipment.

Test Equipment

Vibrations were generated by an electrical vibration exciter that was mounted on a steel rod running through two polytetrafluoroethylene

(Teflon) rings. On the other end of the rod, there was a force transducer and a circular steel plate, 84 mm in diameter, placed on the sand bed. The rod could move freely in the vertical direction, allowing the plate to sink into the sand while it was being compacted. The total mass of the vertically moving system was 37.4 kg, of which 1.16 kg consisted of the vibrating table with added mass. The exciter was controlled by an amplifier and a function generator, making it possible to control both f and amplitude. By analyzing and plotting measured vibrations on the moving mass in real time, the amplitude could be adjusted so that v_0 was kept constant in each test. Because of the great difference between the two masses in the system, vibrations on the moving mass were independent of the dynamic soil response and thus unaffected by resonance in the compactor–soil system. The maximum u_0 of the exciter limited the lowest f to 15 to 20 Hz depending on v_0 for each test. The upper f was limited by the amplifier to 100 Hz for the highest v_0 and 1500 Hz for the lowest v_0.

One accelerometer was mounted on the moving mass of the exciter (A1), and one on the casing (A2). Whereas A1 was independent of soil response, A2 was affected by resonance in the soil–exciter system, producing amplified vibrations at f_r. The setup can be considered as a coupled mass-spring-dashpot system consisting of two masses, the moving mass on the top and the exciter-rod-plate mass on the bottom. The soil may be considered as a spring and a dashpot, connected to the bottom mass. Acceleration signals from both accelerometers were integrated in the amplifiers to evaluate v. A force transducer was mounted above the plate (F1) to obtain the dynamic force with which the soil was loaded. A linear variable differential transformer (LVDT) was connected to the fixed steel frame and the moving rod to measure the vertical displacement of the plate, u_{LVDT}. Several geophones were placed in the sand, on the box perimeter and on the concrete floor, outside the box (G1–G5). These were intended both for the control of resonances and interference patterns in the soil and as sensors for measuring the Rayleigh wave speed c_R. The geophones were placed so that vibrations in different parts of the box were measured and so that c_R measurements could be performed over the compacted area (Fig. 1). A vertical accelerometer was buried in the sand below the plate at a depth of 20 cm (BA1). The depth was selected so that the accelerometer would not significantly influence the compaction result (approximately 2.5 times the plate diameter) and would not be greatly affected by the reflections at the stiff concrete floor (10 cm from the floor). The equipment is summarized in Table 1.

TABLE 1—*Test equipment and labels.*

Equipment	Label	Type
Vibration exciter		B&K PM 4808
Exciter amplifier		TPO300
Function generator		HP 3314 A
Data acquisition		MC USB1616FS
Accelerometer	A1, A2	B&K 4332
Accelerometer	BA1	ADXL250
Accelerometer amplifier		B&K 2635
LVDT	LVDT	Schaevitz RAG
LVDT amplifier		Schaevitz DTR-451
Force transducer	F1	Kistler 9051
Force transducer amplifier		B&K 2635
Geophone	G1-G5	SM 4.5 Hz

Sand Properties

Washed and dried sand was used for the tests. The water content was less than 0.25 %. The range of particle size distribution is shown in Fig. 2. The material was medium-graded, and because there was some separation during transport, the sand was slightly coarser at the very top of the sack (lower boundary in Fig. 2). This problem was overcome by mixing the sand prior to the experiments.

Preparation and Test Procedure

Sand was poured into the box to fill it. The uncompacted density is strongly affected by the sand filling method, as reported by Rad and Tumay (1987). In order to estimate the density ρ before compaction, it was measured in two test preparations by placing seven small containers of varying size and shape in the test box. After the sand was poured, the containers were carefully excavated and weighted. A total of 14 containers showed that the density varied between 1629 kg/m^3 and 1683 kg/m^3 with an average of 1655 kg/m^3. The variations were sufficiently small for the sand to be considered homogeneous for the tests. The sand was poured by the same person, and thus the pouring technique was similar, for all test preparations.

After a layer of 10 cm had been poured, a buried accelerometer was placed at the center of the box and connected to a threaded rod to keep it in place. Once the sand had been poured to its final height
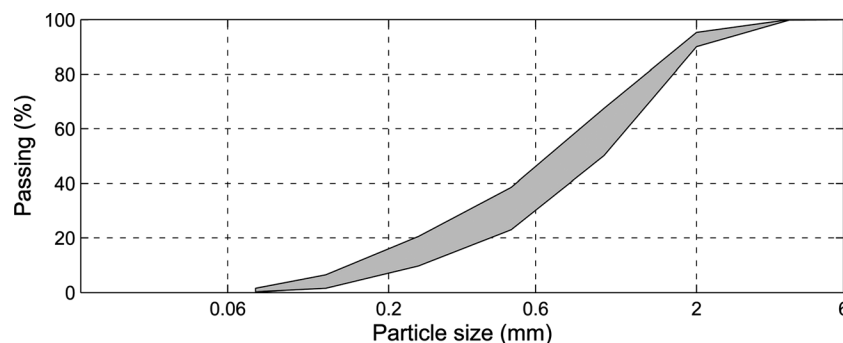

FIG. 2—*Particle size distribution of the test material.*

of 30 cm, the rod was disconnected from the accelerometer and pulled out of the sand. The surface at the center of the box was then preloaded by a static mass of 72 kg with an area of 205 mm × 250 mm (corresponding to a stress of 13.8 kN/m²). The reason for preloading was to get less variation in the initial (uncompacted) ρ between tests. Before and after compaction, c_R between geophones G1 and G2 was measured by impacting a steel plate. The plate was placed 20 cm from G1 and 40 cm from G2 (Fig. 1). The Rayleigh wave was then generated via vertical impact of a rubber hammer on the impact plate, generating a wave propagating through G1 and G2 (at a distance of 20 cm from each other). By observing the first arrival of the Rayleigh wave, an average of c_R was obtained for the sand volume surrounding the vibrating plate.

The exciter was operated with linear (and in some cases logarithmic) frequency sweeps, with a lower boundary at 15 to 20 Hz and an upper boundary at 100 to 1500 Hz depending on the test conditions, as described above. During each frequency sweep, the v_0 on the moving mass of the exciter (A1) was kept constant. Because P is proportional to $v_0{}^2$ (Eq 5), the vibration energy per unit time propagating into the sand was constant with varying f. This facilitated investigation of the frequency dependence at a constant P input.

Evaluation Method

In addition to direct observations of measured data, some evaluation was done based on dynamic relationships for vibrating foundations. In order to analyze and evaluate the test results, it was assumed that the soil could be modeled as a spring and dashpot. Expressions for the dynamic spring stiffness k of a vertically vibrating foundation have been derived for an elastic half-space by Lysmer and Richart (1966). When applying these expressions, it is important to consider strain-dependent moduli (strain softening). Shear and compressive moduli decrease with γ (Hardin and Drnevich 1972; Vucetic and Dobry 1991; Massarsch 2004; Johnson and Jia 2005) and thus with vibration amplitude. Massarsch (2000) argued that shear strain softening is closely related to the rearrangement of particles. That means that the lower threshold of γ for when the shear modulus G starts to decrease is close to the lower threshold for particle rearrangement. Thus, in dynamic loading of the soil, G is constant in the lower amplitude range (i.e., when no compaction takes place) and starts to decrease when the amplitude is sufficient for the soil to be compacted. This concept has not previously been verified experimentally with regard to soil compaction. To investigate strain softening, one may analyze f_r instead of G. The relation between these parameters is presented in the following equations. The expression for k of a vibrating rigid footing on an elastic half-space can be calculated using Eq 6, according to Lysmer and Richart (1966).

$$k = \frac{4 G r_0}{1 - \upsilon} \qquad (6)$$

where:
$r_0 =$ diameter of the footing, and
$\nu =$ Poisson's ratio of the soil.
Further, f_r of a mass-spring-dashpot model is expressed by Eq 7.

$$f_r = \frac{\omega_n}{2\pi} \sqrt{1 - 2\zeta^2} \qquad (7)$$

where:
$\omega_n =$ circular natural frequency, and
$\zeta =$ damping ratio.
The circular natural frequency ω_n is determined using Eq 8, in which m is the static mass.

$$\omega_n = \sqrt{\frac{k}{m}} \qquad (8)$$

Combining Eqs 6–8 shows that f_r is proportional to the square root of G. Because the shear wave speed c_S is also proportional to the square root of G, f_r is proportional to c_S. This relation may be used when evaluating the threshold value for strain softening. Another convenient relation that may be taken advantage of is that γ is proportional to v. Thus, in a comparative analysis in which the exact magnitude of γ is not important, one may observe the influence of v without having to determine γ.

Experimental Program

This paper presents results from 85 tests divided over six test series under varying conditions. The tests were carried out so that v_0 on the moving mass of the vibrator was kept constant while f was varied, either from low to high or from high to low. Sand was not replaced between the tests in each series. Between test series, however, the test box was emptied and refilled. The test series are summarized in Table 2. Test series A was done to get initial results and to verify the optimal test procedure. The main results were obtained from test series B, C, and D. The purpose of test series E and F was to investigate the ratio between compacted and displaced soil to verify that the sand was truly compacted.

Soil Displacement

A crucial consideration is whether the soil is really compacted or merely displaced. This was investigated in test series E and F, each conducted in a small box, measuring the difference between the compacted and uncompacted volumes. The test assumptions are shown schematically in Fig. 3. The area of the plate, multiplied by u_{LVDT}, is illustrated by the dashed lines. It is considered as the sum of the reduction in sand volume due to compaction (henceforth referred to as the compacted volume) ΔV_c and the volume of the heave (displaced volume) ΔV_d. It is thus assumed that all soil being displaced horizontally manifests as heave, neglecting any horizontal compaction that might occur outside the plate. Heave is illustrated by the dotted lines. The tests were performed in small boxes that were filled with sand and embedded within the greater sand volume in the main test box (see Fig. 4). In that way, some wave energy could radiate through the thin walls of the smaller box while the weight of the sand in the box remained constant. The compacted volume ΔV_c was obtained by determining the sand volume in the box before and after compaction. After ΔV_c and $(\Delta V_c + \Delta V_d)$ had been determined, ΔV_d could be calculated. It was thus possible to calculate the ratio of displaced and compacted volume, $\Delta V_d/\Delta V_c$.

In test series E, a box with inner dimensions of 130 mm × 130 mm × 130 mm was filled with sand that was moderately

TABLE 2—*Description of the six test series.*

Test Series	Number of Tests	A1	A2	LVDT	F1	G1	G2	G3	G4	G5	Frequency Sweep	Description
A	19	x	x	x	x		x				Low–high/ high–low	Initial test in a smaller container under varying conditions to provide tentative results and information regarding optimal test procedure.
B	12	x	x	x	x	x	x	x	x		Low–high	Full-size box, gradually increasing amplitude between tests, varying speed of frequency sweep.
C	25	x	x	x	x	x	x	x	x		Low–high	Repetition of test series B with more tests and smaller amplitude increment between tests.
D	16	x	x	x	x	x	x	x		x	Low–high	Constant speed of frequency sweep. Amplitude was increased between each test in the first half of the series and then gradually decreased.
E	8	x	x	x	x						Low–high	Compaction in a small container, 130 mm × 130 mm × 130 mm, placed in the full-size box and embedded in sand.
F	5	x	x	x	x						Low–high	Like test series E, but the size of the container was 115 mm × 115 mm × 63 mm ($W \times L \times H$).

compacted with the 84 mm diameter plate. The test series resulted in $\Delta V_d/\Delta V_c = 0.21$, corresponding to 83 % of the total volume change below the plate resulting from soil compaction. In the second test series, a smaller box was used, with dimensions of 115 mm × 115 mm × 63 mm ($W \times L \times H$), and the sand was heavily compacted. This test series resulted in $\Delta V_d/\Delta V_c = 3.1$, corresponding to 23 % of the volume change resulting from compaction. It is likely that large-amplitude tests give rise to soil failure, with the result that a greater soil volume is displaced, causing heave. Moreover, there is less material that can contribute to ΔV_c. The results from test series E and F verify that the sand was being compacted in the smaller boxes. This suggests that compaction also took place in the main test series conducted in the larger sand box. However, for large v_0, a significant amount is also displaced, and it is assumed that this also applies to tests in the larger box. Results shown in the next section suggest that the main test series (B–D) are comparable to the series using smaller boxes (E and F).
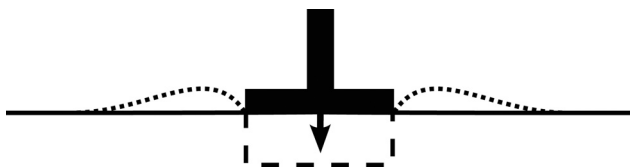
Results

The results of the 85 tests were very similar but varied slightly with v_0. In this section, selected representative tests are presented in detail, particularly one low-amplitude test (C003) and one high-amplitude test (C023). General observations regarding all the tests are also presented.

Figure 5 shows the response of the accelerometers, force transducer, and LVDT in test C003 (small amplitude), in which the v_0 on accelerometer A1 was kept constant at 3 mm/s. Resonance of the compactor–soil system can be clearly observed in accelerometer A2 and force transducer F1, with a maximum at 54 s. Because vibrations are transmitted to the LVDT, very small displacements could not be detected without filtering data. The original data are shown in gray, and the black curve shows data smoothed by a fourth-order Savitzky–Golay filter (Savitzky and Golay 1964). Although the total u_{LVDT} was only 0.0074 mm, a distinct increase in u_{LVDT} was observed at f_r. The same was observed in all tests, regardless of v_0. In Fig. 6, showing the normalized displacement
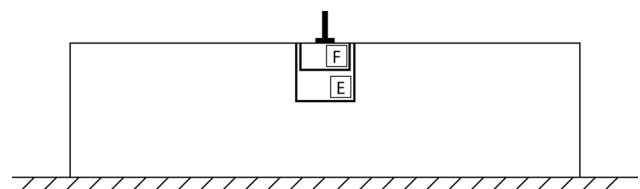

FIG. 3—*Schematic illustration of compaction and heave. The area shown by the dashed lines is the sum of the compacted and displaced volumes, $\Delta V_c + \Delta V_d$, and the dotted lines show soil heave (displaced volume), ΔV_d.*

FIG. 4—*Test series E and F. In each test series, a small box was embedded in the sand.*

FIG. 5—*Response of accelerometers, force transducer, and LVDT in test C003 (small v_0).*
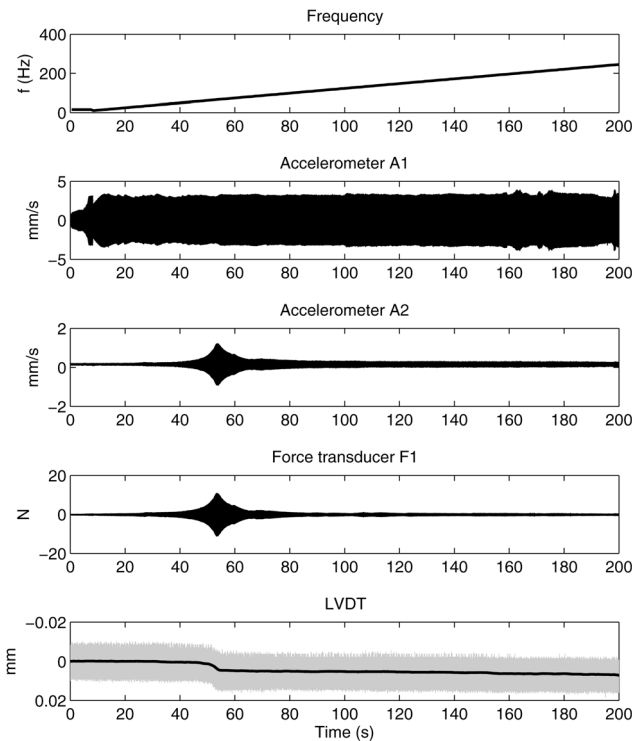
FIG. 7—*Response of geophones and buried accelerometer in test C003 (small v_0).*

velocity of the LVDT versus *f*, the increase in the rate of u_{LVDT} at resonance is even more clearly visible. The frequency at which the largest deformation occurs (here, 66 Hz) is identified as f_r (Nagappagowda and Thulasiram in press). The response of the geophones and the buried accelerometer is shown in Fig. 7. Resonance of the compactor–soil system is clearly observed in G1 and G2 (10 cm from the center of the plate) but is hardly detectable in G3 (30 cm from the plate) and G4 (on the boundary). The geophone behavior contains both amplification and reduction of the amplitude. This is most likely because of the interference of waves and has been observed by other researchers in field measurements where no boundaries were present (Genberg and Bergh Hansson 2002). However, the boundaries might also have affected amplifi-
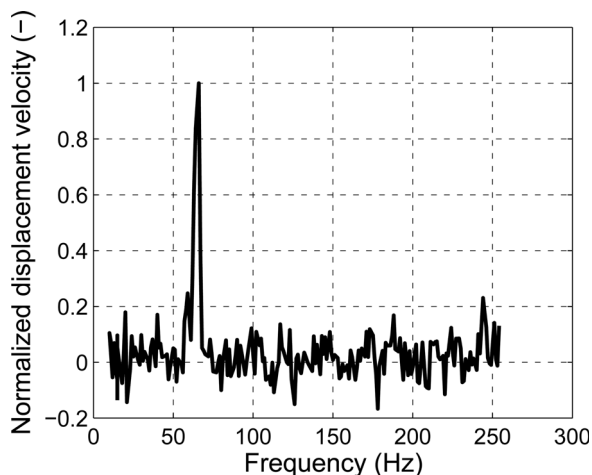
cations and reductions in the present study. BA1 did not react significantly to resonance in any test, suggesting that the resonant amplification was rather local below and around the plate. If the whole sand layer had been in resonance, it would have been clearly visible in BA1. The observation also verifies that the sand layer can, dynamically, be considered as a half-space.

Results from test C023 (large amplitude) are shown in Fig. 8 and Fig. 9. Here, too, resonance is clearly observed with distinct settlement at f_r where u_{LVDT} was 8.7 mm. The normalized displacement velocity is presented in Fig. 10, together with the small-amplitude test described above for reference (Fig. 6). A greater v_0 generally implies a wider peak in the curve of displacement velocity versus frequency.

The tests showed high repeatability; that is, it was possible to accurately obtain the same results in two tests performed under the same conditions. Figure 11 shows v_{LVDT} for the 66 tests in series B–F. Test series A, which was conducted under different conditions (smaller container) with less controllability, is considered as less representative for the general results and has thus been omitted. The distinct increase in v_{LVDT} that was observed in the results presented above is also visible here. It is concluded that all tests yielded similar results. Higher amplitude generally implies higher v_{LVDT} and a wider peak. Because tests were conducted under different frequency sweep speeds, there are slight variations in v_{LVDT}. Test series B–D are shown in gray, and series E and F in black. The similar shapes and locations of the peaks suggest that the confinement of the small boxes in series E and F did not influence the dynamics of the tests considerably. However, the settlement rate was smaller because of the restricted displacement caused by the box boundaries.
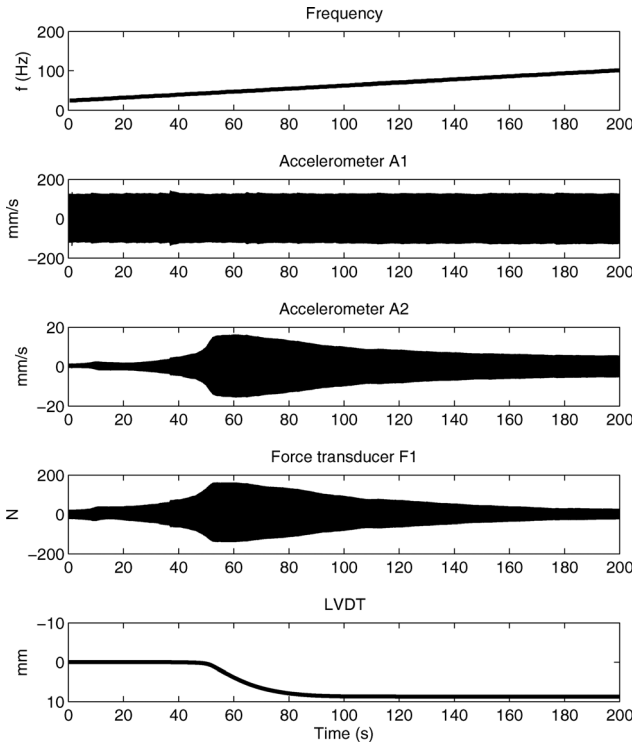

FIG. 6—*Displacement velocity of LVDT in test C003 (small v_0).*

FIG. 8—*Response of accelerometers, force transducer, and LVDT in test C023 (large v_0).*
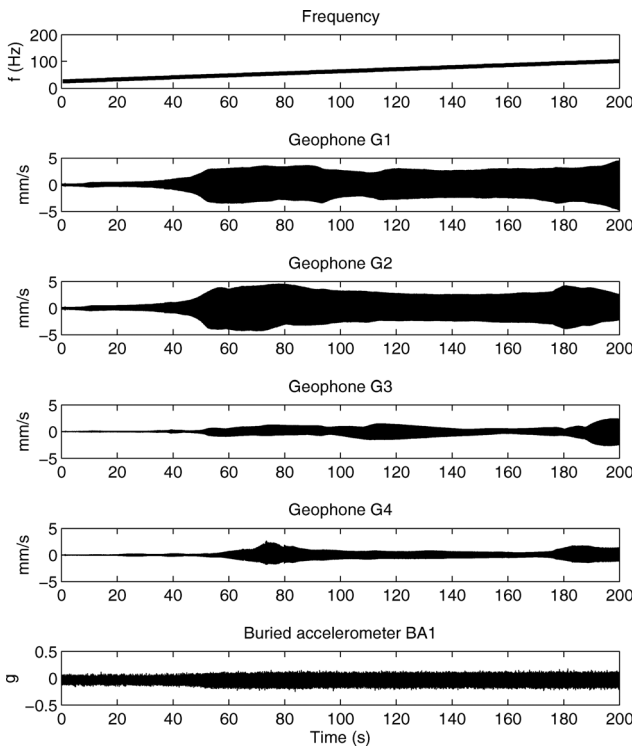

FIG. 9—*Response of geophones and buried accelerometer in test C023 (large v_0).*
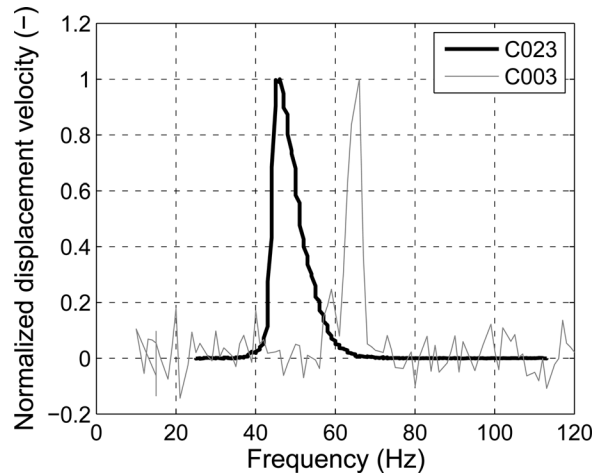

FIG. 10—*Normalized displacement velocity of large-amplitude test (C023) and small-amplitude test (C003).*

secutive tests with identical v_0 (16 mm/s) were performed. The material had previously been dynamically loaded with very small amplitude and was thus considered uncompacted. Tests B004 and B005 had similar sweep speeds. However, the final f was higher in B005 (819 Hz) than in B004 (353 Hz). Both tests started at 20 Hz. In test B006, f was swept logarithmically from 15 to 1017 Hz, producing a very slow sweep around f_r (59 Hz). The applied frequency functions and the displacement velocity of the LVDT, v_{LVDT}, are shown in Fig. 12. Because the material was uncompacted before the commencement of B004, that test produced larger values of v_{LVDT} than the subsequent tests. The figure shows that f_r was identical in all tests, thus verifying that frequency sweep speed does not significantly influence the results.

Measurement of c_R before and after compaction was carried out in the three main test series (B, C, and D). In test series C and D, c_R increased from 113 m/s to 137 m/s and from 131 m/s to 140 m/s, respectively. In test series B, c_R decreased from 130 m/s to 120 m/s. The increment ratios (the ratios of c_R after and before compaction) for test series B, C, and D were 0.92, 1.21, and 1.07, respectively. An increase in c_R is an indication that the soil below the plate is becoming stiffer as a result of compaction. However,
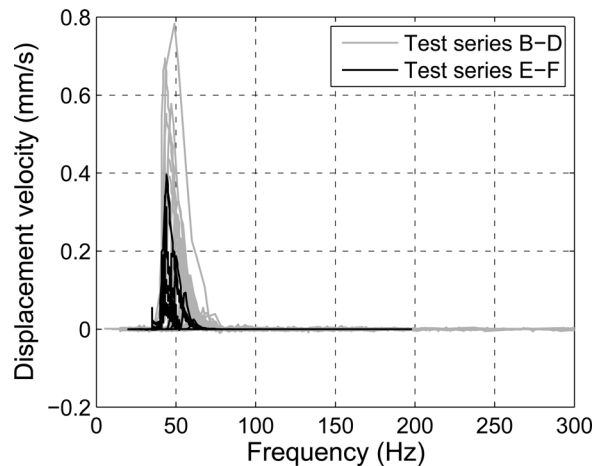

FIG. 11—*Displacement velocity of all tests in series B–D (gray) and series E and F (black).*
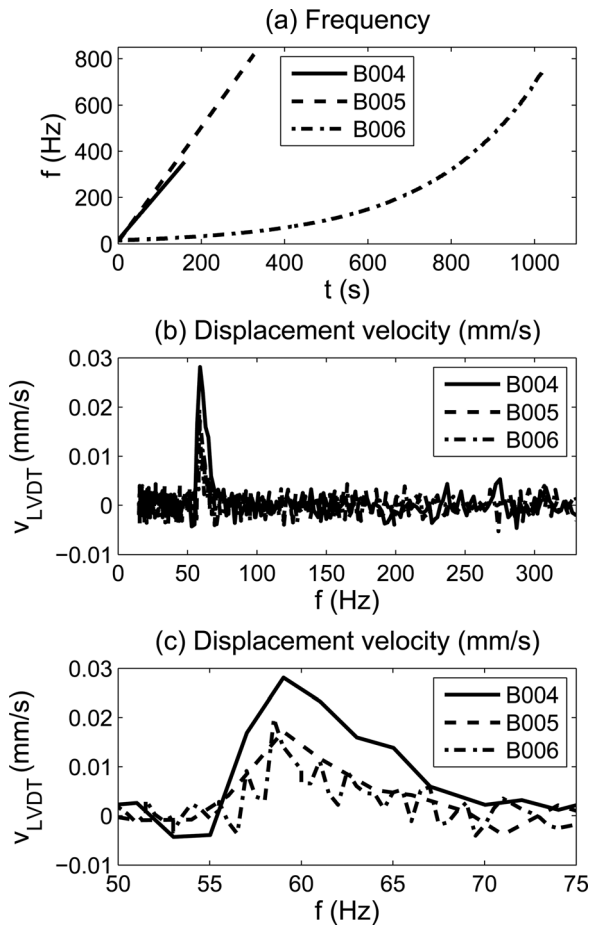
(a) Frequency

(b) Displacement velocity (mm/s)

(c) Displacement velocity (mm/s)

FIG. 12—*Comparison of tests B004, B005, and B006, with the same v_0: (a) the shapes of the frequency sweep curves; (b) v_{LVDT} versus f; and (c) an enlargement of (b) around f_r.*

the increase in c_R is not a good measure of the compaction-induced increase in ρ below the plate because it represents an average over a larger volume of soil than that being compacted. Furthermore, soil displacement and heave might cause the geophones to displace slightly, making the interpretation of c_R more complex. This might be the reason for the decrease in test series B, not necessarily implying a decrease in stiffness. Another measure of greater stiffness below the plate as a result of compaction is the increase in f_r. This is observed in Fig. 13, which shows results from test series D, starting at a low, gradually increasing v_0 and then gradually decreasing. After reaching peak v_0 and with the amplitude again lowered, f_r increases, implying that the sand has become stiffer. This is further confirmation that the sand was being compacted during the tests.

Strain Softening

When the depth of the soil layer is greater than 2.5 to 3 times the plate diameter, the response of the plate is approximately equal to that of a half-space, as has been found in several studies (Baidya and Murali Krishna 2001; Mandal and Baidya 2004). In the present test, the plate diameter was 84 mm and the sand depth was 300 mm. Thus, the response can be approximated as the half-space response. As described above, f_r is proportional to c_S and
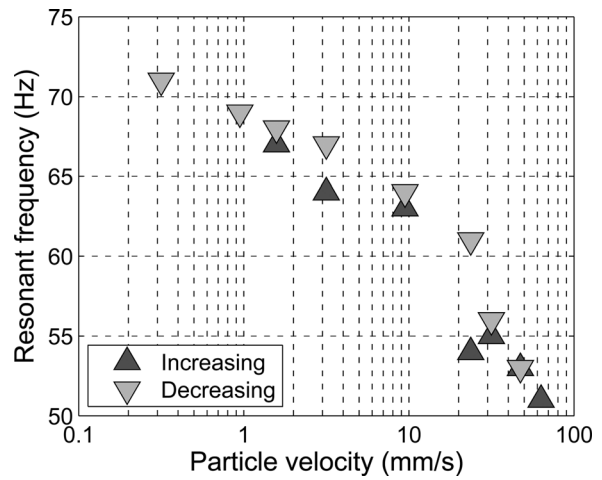

FIG. 13—*Test series with increasing and then decreasing v_0 between tests. The resonant frequency was increased after compaction.*

the square root of G (Eqs 6–8), which implies that f_r is affected by strain softening. Because v is proportional to γ in the sand, f_r is reduced with increasing v, as c_S is with increasing γ. The strain softening effect is shown in Fig. 14(a). Each data point represents results from one test, with f for the largest v_{LVDT} considered as f_r, and different markers show data from the three main test series (B, C, and D). As expected, greater v_0 implies reduced f_r. It can also be observed that the evaluated f_r differs initially in the different test series, probably because of the slightly varying initial density, but it becomes similar as the material is compacted. Figure 14(b)
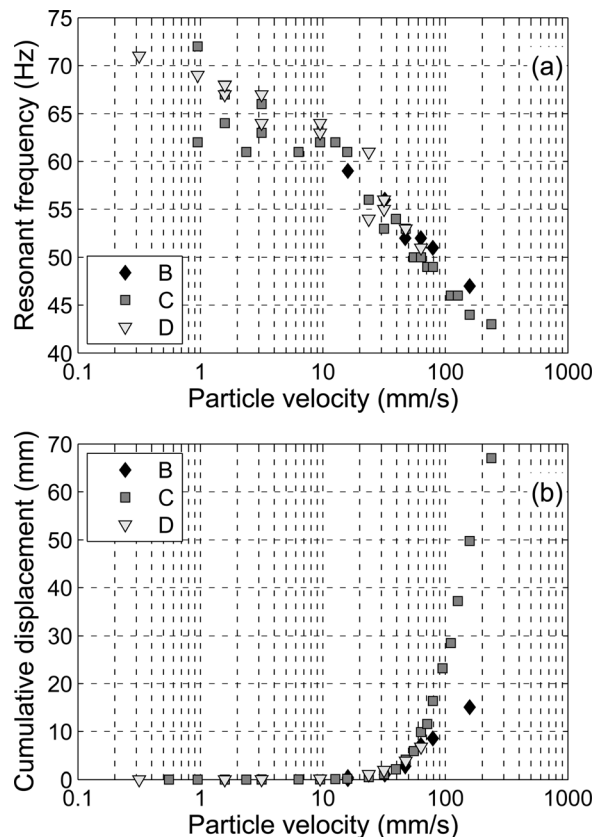

FIG. 14—*Strain softening and cumulative displacement with increasing v_0.*

shows the corresponding cumulative displacement of the plate with increasing v_0 (γ). Considerable displacement occurs at v_0 above approximately 20 mm/s, which is also the threshold for when f_r starts to decrease significantly. This observation confirms that the soil particles are being rearranged above this strain level, as discussed above. Below this value, the settlement is negligible.

Discussion

With the present test setup, it was possible to effectively utilize resonant amplification to compact sand (i.e., to obtain more efficient compaction close to f_r). All tests showed a significant increase in v_{LVDT} at a distinct f. At the same f, vibration and force sensors on, or close to, the vibrating system showed resonant amplification. The conclusion is thus that compaction was significantly improved at f_r. However, larger v_0 caused settlement in a slightly wider frequency interval (Fig. 10). This might have been caused by local bearing failure in the soil in the large-amplitude tests, also resulting in increased heave at the surface near the plate. It might also partly have been caused by loosening of the sand adjacent to the plate because of a lack of confinement. However, the significant amount of heave suggests that the soil was mainly displaced, rather than loosened. The test series intended for investigating soil displacement (E and F) resulted in a greater amount of displacement (compared to compaction) at larger v_0, supporting this hypothesis. Neither the geophones further from the plate nor the buried accelerometer showed significant amplification at the compactor–soil f_r (Figs. 7 and 9). This suggests that the resonance phenomenon was rather local around the plate and that the size of the test box was sufficiently large for the boundaries not to have great influence. Constant-input v_0 proved to be effective when investigating frequency dependence. The shape of the displacement curves, with distinct settlement at resonance and a rapid decrease in settlement rate as f moved above or below f_r, suggests that v_0, rather than u_0 or a_0, is the governing amplitude parameter for the compaction of granular soil. However, this statement has not been confirmed by tests with constant u_0 or a_0.

Discussion in the Context of Roller Compaction

The results indicate that f has a significant influence on the efficiency of vibratory soil compaction. If surface compactors could operate close to f_r of the compactor–soil system, the compaction effect might be increased considerably. However, loading conditions in the present investigation are different from those for roller compaction. The dynamic force is smaller than the static weight, reaching a maximum of 70 % of the compactor weight in the high-amplitude tests. Rollers, on the other hand, have a dynamic force that is considerably larger than the static weight. More efficient compaction is obtained if the dynamic force is larger than the static weight and the compaction equipment is in a state of jumping (Muro and Tran 2006). Furthermore, rollers operate at a certain speed and load the surface with a cylindrical drum, as opposed to the circular plate used in this study. Compaction is normally carried out at optimum water content. Dry sand was used in the present small-scale tests, and it remains to be investigated whether the significant frequency dependence also applies to soil at optimum water

content. Further small-scale and full-scale tests are required in order to investigate how the concept can be applied to roller compaction.

In the manufacturing process of rollers, other considerations related to frequency, such as resonance in machine parts and the vibration effect on the driver, also need to be taken into account. If the aspects described above could be considered while f was allowed to be adjusted to specific conditions, it is probable that roller compaction could be made more efficient. There are two options in applying frequency-dependent compaction, either frequency-variable or fixed but project-specific. The first option implies adjusting f continuously based on dynamic measurements. The concept has been successfully applied in the deep compaction of natural sand and fill utilizing resonant amplification (Massarsch and Fellenius 2002). The second option is to have a fixed f, although differing between rollers, thus making it possible to choose a roller with a certain f. A roller suitable for project conditions can then be selected.

Conclusions

Small-scale compaction tests were performed on dry sand with a vertically vibrating plate. The following conclusions can be drawn from the study:

- The small-scale tests effectively facilitated investigation of the frequency dependence of the compaction of dry sand in the present setup.
- There is a distinct frequency dependence allowing the soil to be more easily compacted close to the resonant frequency.
- Larger vibration amplitude results in compaction in a wider frequency span, but also more soil displacement and heave due to local bearing failure.
- A constant input particle velocity facilitates the investigation of frequency dependence at a constant energy input per unit time, and the test results indicate that it is a crucial compaction parameter, as opposed to displacement or acceleration.
- Strain softening is clearly visible through the reduced resonant frequency at larger amplitudes. Compaction and rearrangement of soil particles are closely related to the strain-dependent reduction of moduli.

The results presented herein need to be verified for other loading conditions and material properties. By performing small-scale tests under different conditions and full-scale tests, the applicability of frequency-dependent soil compaction to vibratory rollers can be investigated. If frequency could be adjusted to current conditions, it is possible that roller efficiency could be significantly improved.

References

Adam, D., 1996, "Flächendeckende Dynamische Verdichtung-skontrolle (FDVK) mit Vibrationswalzen [Continuous Compaction Control With Vibratory Rollers]," Ph.D. thesis, University of Vienna, Vienna, Austria (in German).

Anderegg, R. and Kaufmann, K., 2004, "Intelligent Compaction With Vibratory Rollers," *Transportation Research Record. 1868*, Transportation Research Board, Washington, DC, pp. 124–134.

Arnold, M. and Herle, I., 2009, "Comparison of Vibrocompaction Methods by Numerical Simulations," *Int. J. Numer. Analyt. Meth. Geomech.*, Vol. 33, pp. 1823–2838.

Baidya, D. K. and Murali Krishna, G., 2001, "Investigation of Resonant Frequency and Amplitude of Vibrating Footing Resting on a Layered Soil System," *Geotech. Test. J.*, Vol. 24(4), pp. 409–417.

Bernhard, R. K., 1952, "Static and Dynamic Soil Compaction," *Highw. Res. Board, Proc. Annu. Meet.*, Vol. 31, pp. 563–592.

Converse, F. J., 1954, "Compaction of Sand at Resonant Frequency," *ASTM Spec. Tech. Publ.*, No. 156, pp. 124–137.

D'Appolonia, D. J., Whitman, R. V., and D'Appolonia, E., 1969, "Sand Compaction With Vibratory Rollers," *J. Soil Mech. Found. Div.*, Vol. 95, No. 1, pp. 263–284.

Dobry, R. and Whitman, R. V., 1973, "Compaction of Sand on a Vertically Vibrating Table," *Evaluation of Relative Density and Its Role in Geotechnical Projects Involving Cohesionless Soils*, ASTM STP 523, ASTM International, West Conshohocken, PA, pp. 156–170.

Facas, N. W., Rinehart, R. V., and Mooney, M. A., 2011, "Development and Evaluation of Relative Compaction Specifications Using Roller-Based Measurements," *Geotech. Test. J.*, Vol. 34, No. 6, pp. 634–642.

Forssblad, L., 1965, "Investigations of Soil Compaction by Vibration," *Acta Polytech. Scand.*, No. 34.

Forssblad, L., 1980, "Compaction Meter on Vibrating Rollers for Improved Compaction Control," *Proceedings of the International Conference on Compaction*, Vol. 2, Paris, France, April 22–24, 1980, Ecole Nationale des Ponts et Chaussées and Laboratoire Central des Ponts et Chaussées, pp. 541–546.

Genberg, T. and Bergh Hansson, T., 2002, "Överföringsfunktioner för Tåginducerade Markvibrationer [Transfer Functions for Train-Induced Ground Vibrations]," M.Sc. thesis, Division of Soil and Rock Mechanics, Royal Institute of Technology, Stockholm, Sweden (in Swedish).

Hardin, B. O. and Drnevich, V. P., 1972, "Shear Modulus and Damping in Soils: Design Equations and Curves," *J. Soil Mech. Found. Div.*, Vol. 98, No. 7, pp. 667–692.

Johnson, A. W. and Sallberg, J. R., 1960, *Factors that Influence Field Compaction of Soils*, Bulletin No. 272, Highway Research Board, Washington, D.C.

Johnson, P. A. and Jia, X., 2005, "Nonlinear Dynamics, Granular Media and Dynamic Earthquake Triggering," *Nature*, Vol. 437, No. 6, pp. 871–874.

Lee, F. H. and Gu, Q., 2004, "Method for Estimating Dynamic Compaction Effect on Sand," *J. Geotech. Geoenviron. Eng.*, Vol. 130, No. 2, pp. 139–152.

Lewis, W. A., 1961, "Recent Research into the Compaction of Soil by Vibratory Compaction Equipment," *Proceedings of the 5th International Conference on Soil Mechanics and Foundation Engineering*, Vol. 2, Paris, France, July 17–22, 1961, International Society of Soil Mechanics and Foundation Engineering, London, England, pp. 261–268.

Lysmer, J. and Richart, F. E., Jr., 1966, "Dynamic Response of Footings to Vertical Loading," *J. Soil Mech. Found. Div.*, Vol. 92, No. 1, pp. 65–91.

Mandal, A. and Baidya, D. K., 2004, "Effect of Presence of Rigid Base Within the Soil on the Dynamic Response of Rigid Surface Foundation," *Geotech. Test. J.*, Vol. 27, No. 5, pp. 475–482.

Massarsch, K. R., 2000, "Settlements and Damage Caused by Construction-Induced Vibrations," *Proceedings of the International Workshop Wave 2000*, Bochum, Germany, December 13–15, 2000, Ruhr-University, pp. 299–315.

Massarsch, K. R., 2004, "Deformation Properties of Fine-Grained Soils from Seismic Tests," *Proceedings of the Second International Conference on Site Characterization, ISC'2*, Porto, Portugal, September 19–22 2004, International Society of Soil Mechanics and Geotechnical Engineering, London, England, pp. 133–146.

Massarsch, K. R. and Fellenius, B. H., 2002, "Vibratory Compaction of Coarse-Grained Soils," *Can. Geotech. J.*, Vol. 39, pp. 695–709.

Mooney, M. A. and Rinehart, R. V., 2009, "In Situ Soil Response to Vibratory Loading and Its Relationship to Roller-Measured Soil Stiffness," *J. Geotech. Geoenviron. Eng.*, Vol. 135, No. 8, pp. 1022–1031.

Muro, T. and Tran, D. T., 2006, "Effects of Vertical Exciting Force of a Tracked Vehicle on the Dynamic Compaction of a High Lifted Decomposed Granite," *J. Terramech.*, Vol. 43, pp. 365–394.

Nagappagowda, R. H. and Thulasiram, P. K. M., "Stiffness of Finite Sand Stratum under Vertical Vibrations," *Proc. Inst. Civ. Eng.* (in press).

Rad, N. S. and Tumay, M. T., 1987, "Factors Affecting Sand Specimen Preparation by Raining," *Geotech. Test. J.*, Vol. 10, No. 1, pp. 31–37.

Rinehart, R. V. and Mooney, M. A., 2009, "Measurement of Roller Compactor Induced Triaxial Soil Stresses and Strains," *Geotech. Test. J.*, Vol. 32, No. 4, pp. 347–357.

Savitzky, A. and Golay, M. J. E., 1964, "Smoothing and Differentiation of Data by Simplified Least Squares Procedures," *Anal. Chem.*, Vol. 36, No. 8, pp. 1627–1639.

Thurner, H. and Sandström, Å., 1980, "A New Device for Instant Compaction Control," *Proceedings of the International Conference on Compaction*, Vol. 2, Paris, France, April 22–24, 1980, Ecole Nationale des Ponts et Chaussées and Laboratoire Central des Ponts et Chaussées, pp. 611–614.

Vucetic, M. and Dobry, R., 1991, "Effect of Soil Plasticity on Cyclic Response," *J. Geotech. Engrg.*, Vol. 117, No. 1, pp. 89–107.

Wersäll, C., Bodare, A., and Massarsch, K. R., 2012, "Vibration Source Localization along Railway Tracks," *Noise and Vibration Mitigation for Rail Transportation Systems: Notes on Numerical Fluid Mechanics and Multidisciplinary Design*, Volume 118, T. Maeda, P.-E. Gautier, C. E. Hanson, B. Hemsworth, J. T. Nelson, B. Schulte-Werning, D. Thompson, and P. de Vos, Eds., Springer, Tokyo, Japan, pp. 267–274.

Xia, K., 2012, "A Large Deformation Finite Element Model for Soil Compaction," *Geomech. Geoeng.*, Vol. 7, No. 2, pp. 123–137.

Yoo, T.-S. and Selig, E. T., 1979, "Dynamics of Vibratory-Roller Compaction," *J. Geotech. Engrg. Div.*, Vol. 105, No. 10, pp. 1211–1231.

Paper II

Frequency Variable Surface Compaction of Sand Using Rotating Mass Oscillators

Wersäll, C., Larsson, S., Rydén, N. and Nordfelt, I.

Frequency Variable Surface Compaction of Sand Using Rotating Mass Oscillators

Carl Wersäll[1], Stefan Larsson[1], Nils Rydén[2] and Ingmar Nordfelt[3]

[1]*Department of Civil and Architectural Engineering, KTH Royal Institute of Technology, SE 100 44, Stockholm, Sweden*

[2]*Engineering Geology, Faculty of Engineering, Lund University, Box 118, SE 221 00, Lund, Sweden*

[3]*Dynapac Compaction Equipment AB, Box 504, SE 371 23, Karlskrona, Sweden*

Abstract

The influence of vibration frequency was studied in 105 small-scale compaction tests, conducted using a vertically oscillating plate. The underlying soil was dry sand, or sand close to the optimum water content. The results showed that there is a resonant amplification, providing a slightly higher degree of compaction. There is no single dynamic quantity that is governing for soil compaction, but rather a combination. Frequency has a major influence. An iterative method for calculating the dynamic response of the plate, incorporating strain-dependent properties of the soil, is also presented. The calculated frequency response agrees well with measured quantities.

Keywords: Compaction, resonance, strain softening, frequency response, vibratory roller

Introduction

Soil compaction using a vibratory roller is governed by highly plastic strains, nonlinear dynamic behavior and, occasionally, chaotic motion. These characteristics make modeling of roller compaction a difficult task. Research on improving compaction efficiency has mainly consisted of full-scale trial-and-error studies and the fundamental process of soil compaction is not wholly understood. To obtain knowledge of a dynamic system, the response of the system to dynamic loading needs to be investigated over a wide frequency span. However, the influence of vibration frequency f on the compaction efficiency has not been fully investigated. In the previous paper by Wersäll and Larsson (2013), it was concluded that very little research has been conducted on the frequency dependence of soil surface compaction and that no experimental studies have been published on the subject since the 1970s. Among the most important advances were early studies by

Bernhard (1952), Converse (1954), D'Appolonia et al. (1969), and Dobry and Whitman (1973). The conclusions of early researchers were, in general, that compaction must be conducted above the coupled soil-compactor resonant frequency f_r. Above resonance, f has influence but there was no consensus among researchers regarding the magnitude of that influence or, in particular, its practical applicability.

Several researchers have studied the dynamic behavior of vibratory rollers. Yoo and Selig (1979) developed a model based on coupled mass-spring-dashpot systems, which has been widely used. Adam (1996) identified, and showed by measurement and simulation, the different modes of roller operation – contact, periodic loss of contact, and chaotic motion. Extensive research has also been done on roller behavior with regard to continuous compaction control (e.g. Forssblad 1980; Thurner and Sandström 1980; Adam 1996; Anderegg and Kaufmann 2004; Mooney and Rinehart 2009; Facas et al. 2011).

Wersäll and Larsson (2013) conducted small-scale compaction tests using a vertical electro-dynamic oscillator. The tests showed that there was a significant frequency dependence resulting in a higher degree of compaction close to f_r. However, the compaction equipment used in those tests was not representative of roller compaction since the dynamic force was significantly lower than the static weight. The purpose of this paper is to present a study of the compaction frequency dependence in small-scale tests with a purpose-built compactor using rotating eccentric mass oscillators and to describe a novel method for calculating the frequency response. This compactor is significantly more similar to a vibratory roller than the previous equipment with regard to dynamic-to-static load ratio. The tests were conducted in order to study the influence of f on the degree of compaction. The influence of w was also investigated by conducting tests on dry sand and sand with w close to its optimum water content (OWC). It is well-known that soil is more easily compacted close to OWC. However, this effect is less pronounced for coarse-grained soils.

Methods and Materials

To investigate the influence of f on the compaction of sand using rotating eccentric mass oscillators, small-scale tests were conducted in a sand-filled box with inner measurements 1100 mm x 700 mm x 370 mm (W x L x H). The test equipment is shown in Fig. 1. Two oscillators (Lofgren Engineering NEG 5020) were mounted on a steel rod that could move vertically but not horizontally. The eccentric masses were counter-rotating, thus producing only a vertical vibration component. An 84 mm

FIG. 1 – *The test box and experimental setup.*

diameter steel plate was connected to the bottom of the rod. A force transducer and a vertical accelerometer were placed above the plate. The total mass of the vertically moving system was 28.8 kg, resulting in 51 kPa static contact stress. In some tests, geophones were placed in the sandbox, on the box's perimeter or on the concrete floor.

Material Properties

The test material consisted of washed sand with d_{60} = 0.9 mm and d_{10} = 0.2 mm. Proctor tests were conducted for w above 3%. The tests showed constant Proctor density for all values of w with a slight increase close to the maximum w (12.3%), which is a typical behavior for free-draining granular soil. The dry sand had a w of less than 0.2%. In the tests with wet sand, a mean value of w of 9% was aimed for. Due to the shape of the Proctor curve, small variations in w were considered to have insignificant influence of the test results. The density ρ of the dry sand was 1655 kg/m^3 on average with a sufficiently small variation.

Test Procedure

Before each test, the box was excavated and refilled with sand. The sand was filled by pouring, using the same procedure to obtain a similar initial ρ in all tests. In the tests where wet sand was used, w was also measured in a number of locations throughout the test box and modified if necessary. After filling, the center of the

3

sand surface was preloaded by placing a 195 mm x 195 mm wooden plate between the steel plate and the surface of the sand and then vibrating the system at 100 Hz for 20 seconds. After preloading, the wooden plate was removed and the system was vibrated at the current f of that test for 30 seconds. The duration was chosen such that the settlement of the steel plate, S, for every tested f was below the maximum S that the system was designed for, i.e. 60 mm. A constant duration implies that the number of cycles and consumed energy is dependent on f but this is also true in the case of roller compaction. During the test, S was measured by a linear variable differential transformer (LVDT), the reaction force F by a force transducer above the bottom plate and the vertical acceleration a by an accelerometer mounted on top of the plate.

Data Evaluation

All measured quantities were analyzed directly in the time domain. Furthermore, the measured a was analyzed in the frequency domain and also integrated to velocity v and displacement u. The static displacement of the LVDT is denoted settlement S to avoid confusion with dynamic particle displacement u. Each test was conducted at a discrete f that was set in the frequency converter. However, due to some frequency lag in the oscillators, the actual f was lower than the nominal value (that specified in the frequency converter). To analyze the correct f, the value obtained by frequency analysis of the measured acceleration signal, rather than the nominal operating value of the frequency converter, was adapted as f of each particular test.

Since the sand below the plate was compacted during the tests, the stiffness increased, changing the measured dynamic signals. There are thus no obvious values to represent the measured and evaluated amplitudes since they varied over time. The root mean square (RMS) was here used to find a representative value. It is often used as an average measure of a periodic signal. The RMS value g_{RMS} of a function g, over a time period t_1 to t_2, is calculated by Eq 1.

$$g_{RMS} = \sqrt{\frac{1}{t_2-t_1}\int_{t_1}^{t_2}|g(t)|^2dt} \qquad (1)$$

Commonly, the RMS is not calculated over the whole signal but rather in short time domain windows, called running RMS. The time window is chosen in relation to frequency so that a sufficient number of oscillations are included in one interval, while still capturing variations of the signal amplitude. For each F, a, v and u time history, the 0.5 second running RMS was calculated. The maximum value of that running RMS was then adopted as a representative value of the amplitude for further evaluation. Since compaction is governed by the magnitude of shear strain γ, where a small increment in strain can have a dramatic effect on the rate of

compaction (Wersäll and Larsson 2013), the maximum RMS is assumed to be more representative than the mean RMS.

Calculation of Frequency Response

There is at present no model for estimating compaction (increase in density) at different f but there are methods to estimate the frequency response (output of the system at different frequencies) of dynamic quantities such as u and a. Nonlinear soil behavior can be estimated by an iterative methodology using empirical expressions, as described below. A further consideration is the response of the finite sand layer in comparison to the calculated response of a half-space, as has been shown experimentally by Mandal et al. (2012).

The displacement frequency response of a single degree of freedom system can be calculated using Eq 2.

$$u_0 = \frac{F_0(\omega)}{k} \frac{1}{\sqrt{(1-\beta^2)^2+(2\zeta\beta)^2}} \qquad (2)$$

where

u_0 = displacement amplitude

F_0 = applied force amplitude,

k = spring stiffness,

β = dimensionless frequency, and

ζ = damping ratio.

The spring stiffness k and damping ratio ζ for a vibrating foundation on a half-space are calculated using Eqs 3 to 5 according to Lysmer and Richart (1966).

$$k = \frac{4Gr_0}{1-v} \qquad (3)$$

$$\zeta = \frac{0.425}{\sqrt{B_z}} \qquad (4)$$

$$B_z = \frac{1-v}{4} \frac{m}{\rho r_0^3} \qquad (5)$$

where

G = shear modulus,

r_0 = plate radius,

v = Poisson's ratio,

B_z = mass ratio, and

m = total mass.

The total mass m is usually assumed to consist of the mass of the foundation and a widely discussed apparent mass. This is not an actual oscillating mass but rather a correction for the decrease in stiffness, observed in measurements of foundation response (Richart and Whitman 1967; Gazetas 1983). Several authors have ignored this correction, as discussed by Susante and Mooney (2008). The calculated apparent mass, using the test properties herein, becomes less than one percent of the foundation mass and is therefore disregarded.

The dimensionless frequency β is the ratio between the circular frequency ω and the natural circular frequency ω_n, according to Eqs 6 and 7.

$$\beta = \frac{\omega}{\omega_n} \tag{6}$$

$$\omega_n = \sqrt{\frac{k}{m}} \tag{7}$$

The applied force amplitude from a rotating eccentric mass vibrator is determined by Eq 8.

$$F_0 = m_e e \omega^2 \tag{8}$$

where

$m_e e$ = eccentric moment, consisting of the eccentric mass m_e and the eccentricity e.

Reduction of G with increasing γ (strain-softening) has been studied by many authors (Hardin and Drnevich 1972a; Vucetic and Dobry 1991; Rollins et al. 1998; Massarsch 2004, among others) and there exist several empirical models for estimating G and ζ at increasing γ. Wersäll and Larsson (2013) showed that modulus reduction is closely related to rearrangement of soil particles and compaction. Hardin and Drnevich (1972b) proposed that G and ζ should be adjusted for γ according to Eqs 9 and 10.

$$\frac{G}{G_{max}} = \frac{1}{1+\left|\frac{\gamma}{\gamma_r}\right|} \tag{9}$$

$$\frac{\zeta}{\zeta_{max}} = 1 - \frac{G}{G_{max}} \tag{10}$$

where

G_{max} = small strain modulus,

γ_r = a reference strain, based on soil properties, and

ζ_{max} = maximum damping ratio.

For clean dry sand, ζ_{max} is 33% in the first loading cycle according to Hardin & Drnevich (1972b). Rollins et al. (1998) developed an approximation for gravel without the use of a reference strain, shown in Eqs 11 and 12.

$$\frac{G}{G_{max}} = \frac{1}{1.2+16\gamma\left(1+10^{(-20\gamma)}\right)} \tag{11}$$

$$\zeta = 0.8 + 18(1 + 0.15\gamma^{-0.9})^{-0.75} \tag{12}$$

Massarsch (2004) proposed an expression for modulus reduction of fine-grained soils presented in Eq 13.

$$\frac{G}{G_{max}} = \frac{1}{1+\alpha\gamma\left(1+10^{-\beta\gamma}\right)} \tag{13}$$

where

α and β are empirically determined parameters depending on plasticity index (PI).

Note that γ in Equations 11-13 above is expressed as a percentage. Furthermore, the equations are here displayed as given in the papers but to be valid even for strains less than zero, the absolute value of γ should be applied instead of the negative value. All models exhibit weaknesses. Eq 9 matches measured data quite poorly and the reference strain is difficult to determine. Eq 11 does not approach unity for very low strains, and hence does not capture the small-strain modulus. Eq 13 is only valid for PI larger than 10% and thus does not include data from tests on granular soils. Eq 2 was used to calculate the theoretical u_0 of the rotating mass system in the frequency domain. To obtain strain-dependent G and ζ, however, u_0 must be converted to γ. This means that the compressive strain ε must first be calculated from u_0 by dividing it by the total length of the strained element. Strain is not evenly distributed but this simplification is, however, necessary. The sand volume which influences the dynamic properties of the system has been found by other authors to extend to a depth of 2.5 to 3 times the plate diameter (Baidya and Murali Krishna 2001; Mandal and Baidya 2004). Since the plate diameter is 84 mm in diameter and the sand depth is 120 mm, the entire depth of the sand can be assumed to affect the system. However, by far the most of influence is obtained from the top part of the sand layer. The simplification of regarding the sand bed as a half-space is therefore assumed to be reasonable, although in reality the underlying concrete has a slight influence on the results. The shape of the strain distribution over depth can be assumed to follow the Boussinesq stress distribution. This is simplified to a triangular distribution over two thirds of the depth of the sand layer, which is further simplified to an evenly distributed strain over one third of the sand depth. Hence, the length of the strained element is considered to be 40 mm. After ε is obtained, γ can be calculated by Eq 14 (for axisymmetric conditions).

$$\gamma = \frac{2}{3}\varepsilon(1 + v) \tag{14}$$

Each point in the response diagram represents a magnitude of γ, which corresponds to a value of G and a value of ζ. After these have been calculated, a new value of γ can be obtained using the procedure above. This is iterated until u_0 converges for every f. The number of iterations is quite small, generally between 5 and 10, which agrees well with the number of iterations required in the similar iteration procedure described by Schnabel et al. (1972). In this study, Eq 13 is used to calculate G even though it is based on empirical data from fine-grained soils. The parameters α and β are chosen for PI = 10 %, which is the lowest PI available for that expression. Stokoe et al. (1999) showed that strain-softening for soils with low PI and for non-plastic soils is very similar. This uncertainty is thus considered to be less significant than the uncertainties in Eqs 9 and 11. The damping ratio ζ is calculated by Eq 10, assuming ζ_{max} = 33%. After iteration, the strain-dependent frequency response for u_0 is obtained, which can be converted to the response for velocity amplitude v_0, acceleration amplitude a_0 or F_0.

Results and Discussion

This section presents the results from 105 small-scale compaction tests conducted using the same procedure, changing only f and w. Dry sand was used in 60 tests and 45 tests were conducted using wet sand with a water content of around 9%. Summaries of all test results, presented with selected quantities, are shown below. Control measurements using geophones showed v_0 up to 10 mm/s in the sand, 25 cm from the plate, and up to 2 mm/s on the concrete floor.

In the small-scale tests described in the previous paper, the correlation between S and compaction was an issue due to observable heave on the sand surface. In the present tests, however, no heave could be observed at the surface in spite of significant S. Fig. 2 shows the bottom plate after end of compaction in a test using wet sand. The depressed square area is the result of pre-consolidation. Since there is no apparent heave it is considered reasonable to assume that S is closely related to compaction, i.e. decrease in volume and increase in density.

Fig. 3 shows an example of a time history of measured vertical a, F, and S in a test of dry sand at 45 Hz. Over the 30-second duration of the test, S nearly reaches its maximum, as can be seen at the bottom of the figure. During roller compaction, most of the achievable settlement, but not all, is cumulated (demonstrated by the fact that increasing the number of passes above what is customary increases the degree of compaction slightly) and the test duration is thus considered to fairly well represent that of compaction by vibratory roller. Since the soil below the plate

8

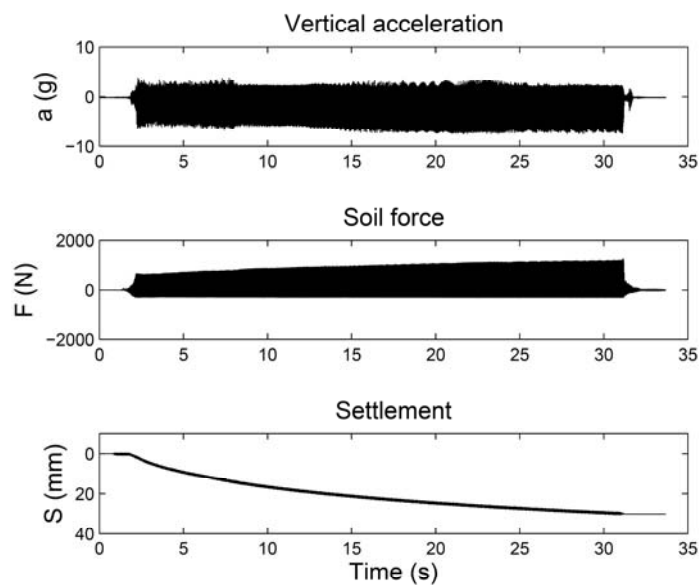FIG. 2 – *End of compaction with no observable heave.*

FIG. 3 – *Vertical acceleration of the plate, reaction force and settlement in a 45 Hz test.*

becomes stiffer as it is compacted, F_0 increases during the test. The constant quantity during the tests was $m_e e$.

Frequency Response

The conventional calculated frequency response, not corrected for strain-softening, of a_0 and u_0 is shown in Fig. 4 for different values of the soil shear wave speed c_S. Eq 2 was used to calculate u_0 while a_0 was obtained by multiplying u_0 by ω^2. The eccentric moment was $m_e e = 3.81 \cdot 10^{-3}$ kgm, which was constant throughout all tests.
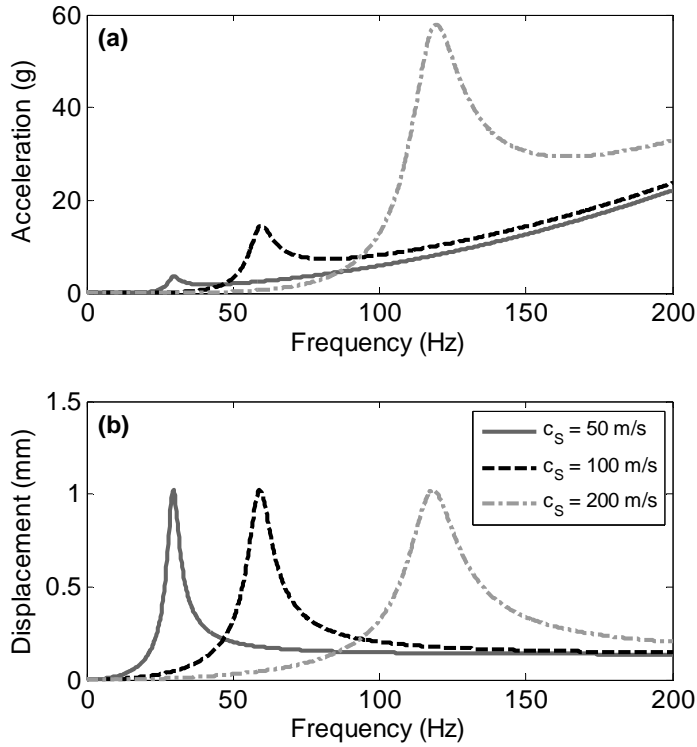
FIG. 4 – *Calculation of acceleration and displacement amplitudes without correction for strain-softening.*

The known quantities r_0 = 42 mm, m = 28.8 kg and ρ = 1655 kg/m^3 (for dry sand) were applied and Poisson's ratio was assumed to be ν = 0.30. The value of a_0 at resonance increases drastically with c_S while it is constant for u_0. The same is true for the amplitudes a_0 and u_0 when f increases well above resonance.

As can be seen from Fig. 4a, a_0 approaches extreme values with high c_S and f due to the significant increase in F_0 with f (Eq 8). In reality, the high γ associated with high loads causes the stiffness of the soil to reduce drastically, implying much lower values of a_0 and u_0, as well as of f_r. When strain-softening is considered, the response displayed in Fig. 4 is therefore dramatically different.

The calculated frequency response, incorporating the effect of strain-softening, is shown below together with respective measured variables. The strain-dependent u_0 response was calculated by Eqs 2, 10 and 13 and iterated until convergence. The quantities a_0, v_0 and F_0 were calculated from the strain-dependent u_0. The shear wave speed in the model was adjusted so that the calculated f_r became identical to f_r of the compactor-soil system, which is apparent from the measured data, i.e. 42 Hz. This resulted in c_S = 200 m/s.

The measured and calculated a_0 is shown in Fig. 5. Considering the many uncertainties, both in the calculation and the test procedures, the agreement is fairly good. Resonance is not clearly visible due to the large degree of damping, resulting in no peak but rather a continuously increasing a_0. Comparing the scales between Fig. 4a and Fig. 5, one can clearly observe how strongly strain-softening affects the dynamics of the system. The tests with wet sand produced slightly higher values of a_0. Fig. 6 shows the corresponding relation for v_0. There is a good correlation up to f_r. Above this frequency, measured values are relatively constant while the calculated values increase.

The particle displacement amplitude u_0 as a function of f for all tests is shown in Fig. 7. The maximum u_0 appears at f_r, 42 Hz. The data, obtained by double integration of measured a, agree with the calculated frequency response but with some scatter. The tests with wet sand follow the same trend as those with dry sand. Fig. 8 shows measured and calculated F_0, which increases rapidly up to f_r and is then fairly constant. The results in the figures above agree well with the u_0-f and F_0-f relationships in Anderegg and Kaufmann (2004), measured during roller operation using a high $m_e e$.
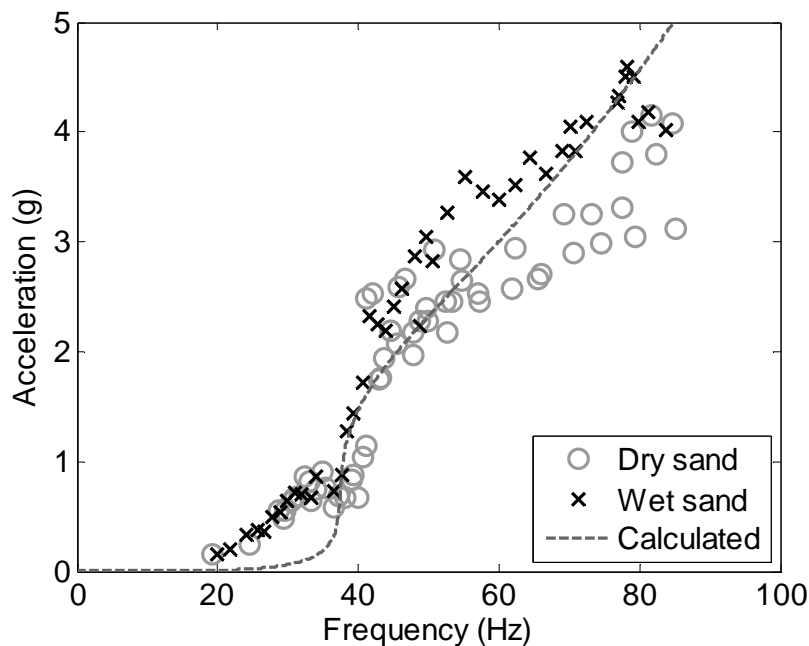

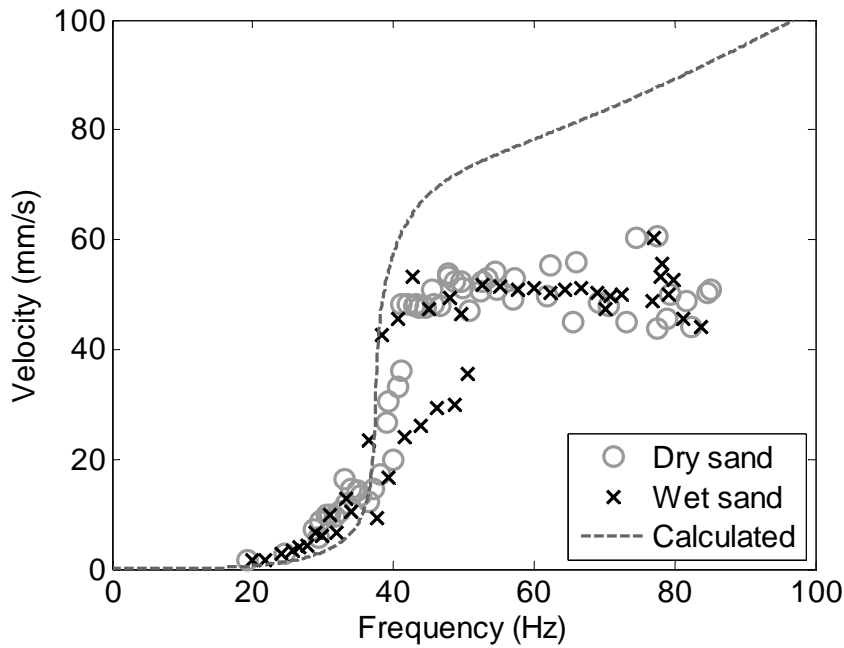FIG. 5 – *Measured maximum RMS value of acceleration amplitude and calculated frequency response.*

FIG. 6 – *Maximum RMS value of particle velocity amplitude from measured and calculated frequency response.*
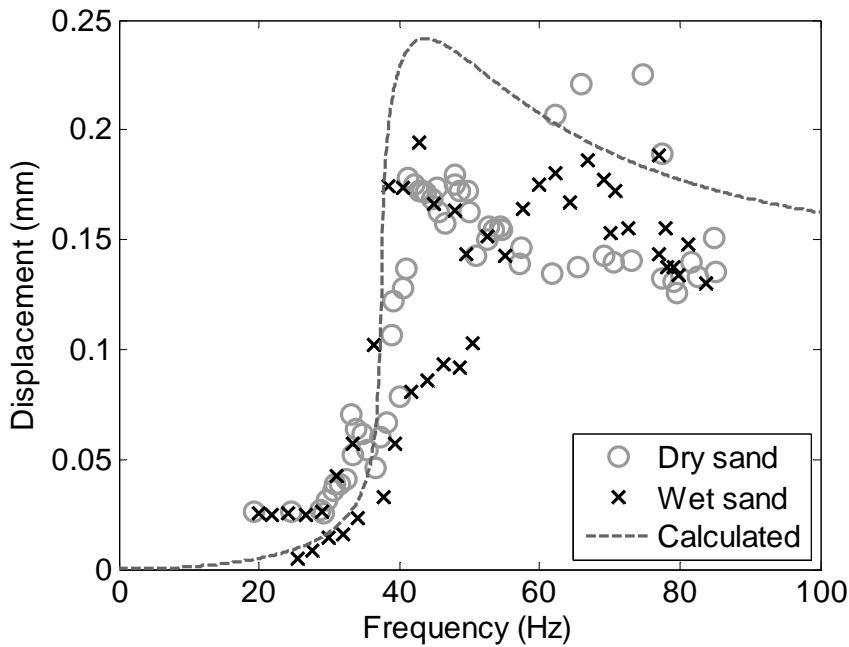

FIG. 7 – *Maximum RMS value of particle displacement amplitude from measurement and calculated frequency response.*
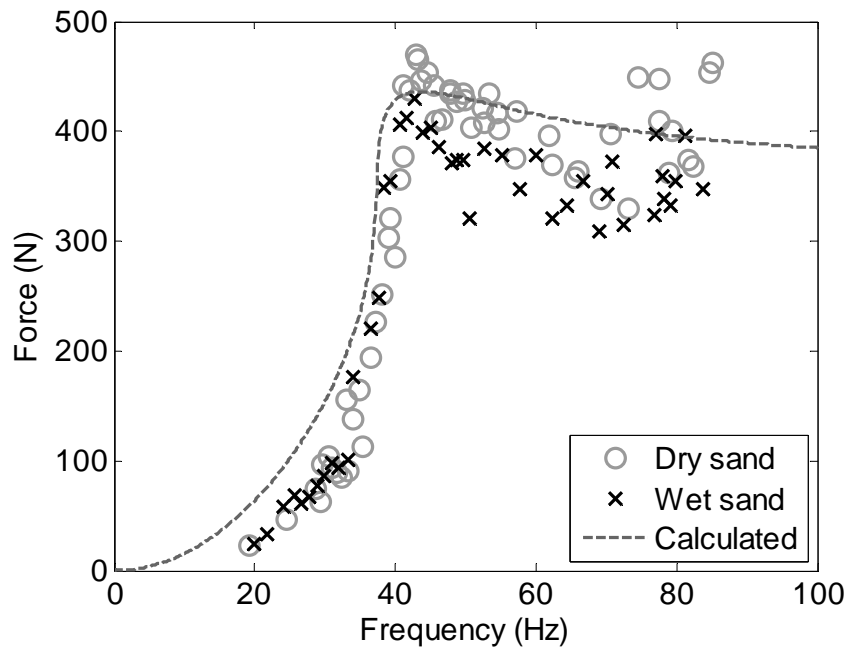
FIG. 8 – *Measured maximum RMS value of force amplitude and calculated frequency response.*

Compaction

The tests provided the opportunity to study the influence of u_0, v_0, a_0 and F_0 on the compaction efficiency in order to determine whether there is a single governing quantity. The previous tests with the electro-dynamic oscillator indicated that v_0 is governing for compaction with such an oscillator. Fig. 9 shows the total S at each test, versus different measured dynamic quantities. In Fig. 9a, S is displayed as a function of maximum F RMS value. Although S increases with higher F_0, the correlation is weak, indicating that there are other parameters that have significant influence, provided the measurement error is small. The same is true for S versus u_0 and v_0, shown in Fig. 9b and c, respectively. The acceleration amplitude a_0, however, has a more obvious influence on S, as can be seen from Fig. 9d. Nonetheless, there is a large scatter and a_0 cannot be solely governing for compaction. These results confirm that there is no exclusive quantity that is essential for soil compaction and that f affects compaction to a large extent. The relationship between compaction and dynamic quantities is, however, complex since the considered quantities are correlated to each other.
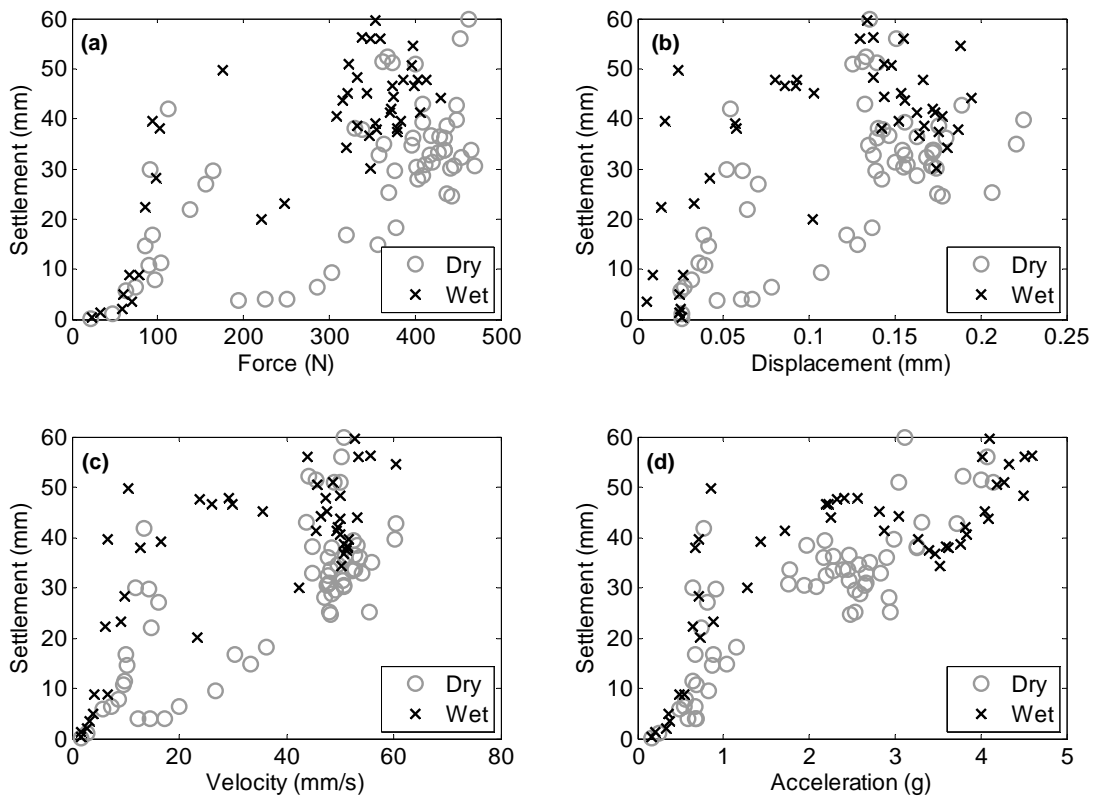
FIG. 9 – *Measured settlement as a function of force, displacement, velocity and acceleration amplitudes.*

The total S, closely related to compaction, is shown in Fig. 10 as a function of f. The results from the tests with wet sand are similar to those with dry sand, except for S being slightly larger, roughly up to 25%. The water content affects c_S, which in turn affects f_r but the results show that the difference in f_r between dry and wet sand is negligible. In a practical regard, w thus only affects the degree of compaction and the effect on the dynamic properties of the soil is insignificant. There is resonant amplification, causing a higher degree of compaction around f_r at 42 Hz.

There are some uncertainties in the results. What appears to be scatter just below f_r in Fig. 10 (approximately 30-40 Hz) is on closer inspection caused by a sudden rapid decrease in settlement around 35 Hz. This is more obvious in Fig. 11 where S has been normalized by the measured F_0. It can be clearly seen that the S-to-F_0 ratio increases up to a certain f and then falls suddenly. This f is below f_r, implying that just below this threshold, the soil is easily compacted by a small F_0 while the opposite is true directly above the threshold. The phenomenon has yet to be explained and is a subject for further study. The explanation might be a nonlinear resonance effect or the transition between different compaction modes (such as contact and loss of contact). Another explanation may be the threshold representing the resonant

frequency of the test box causing the whole box to oscillate above the threshold while acting as a rigid body below. What is clear, however, is that in this frequency region, the degree of compaction obtained is highly variable.
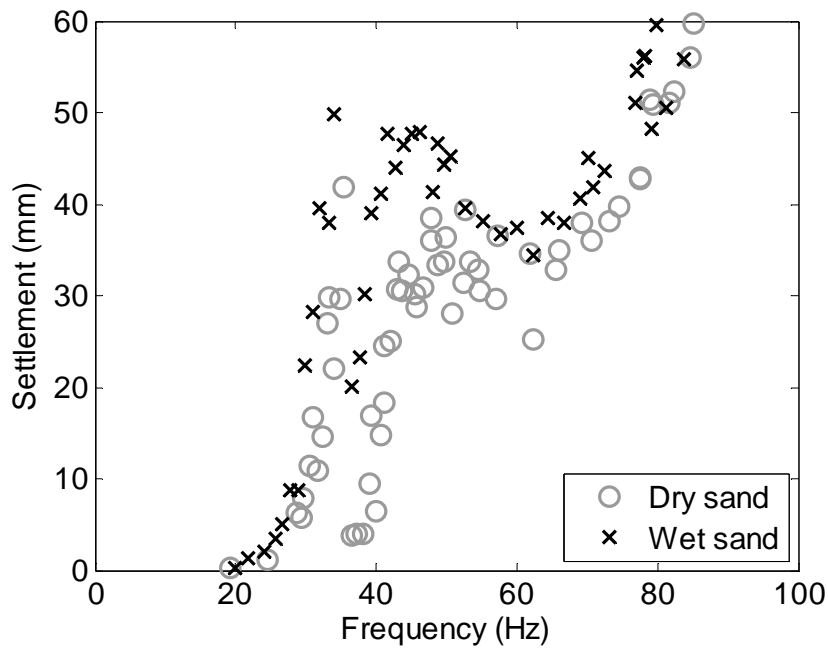

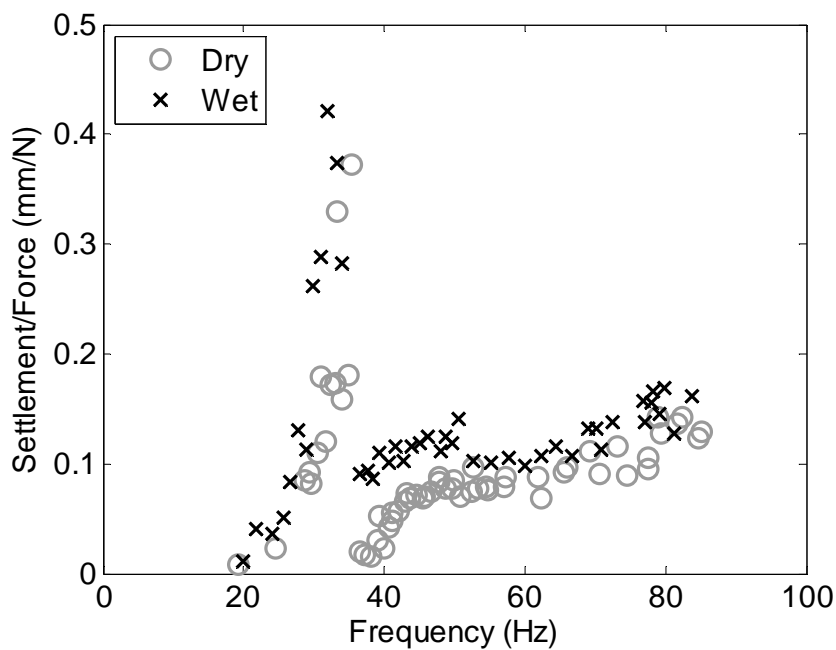
FIG. 10 – *Settlement of dry and wet sand.*

FIG. 11 – *Settlement normalized by force amplitude.*

Discussion in the Context of Roller Compaction

In a practical regard, the degree of compaction can be divided into four different frequency ranges, shown schematically in Fig. 12 together with the above test results. Range I, very low f, gives S close to zero, i.e. no compaction in addition to the static compaction. In Range II, the achieved degree of compaction is increases rapidly, but it is not recommended to operate within this range since the compaction effect is very variable, as discussed above. Range III contains the frequencies directly above resonance, where the degree of compaction decreases slightly as f is increased. In Range IV, high f, it again increases rapidly.

From Fig. 12 it would seem that Range IV is the optimal for roller compaction and that a high f is more favorable. However, if the compaction aspect is disregarded, there are machine-related disadvantages to operating at a high f. Most obvious is the increased wear to machine parts, e.g. the hydraulics. The lifespan of the vibrator is also shortened as it depends on the total number of cycles. Furthermore, a high f will increase fuel consumption and emissions. It is thus favorable not to operate at a higher f than necessary.

The coupled roller-soil f_r depends on machine and soil properties and is often not known. Full-scale tests must be conducted to determine where roller operation takes place in relation to the frequency ranges in Fig. 12. If f is at the high end of Range IV, lowering f would imply a reduced compaction effect. However, if the roller
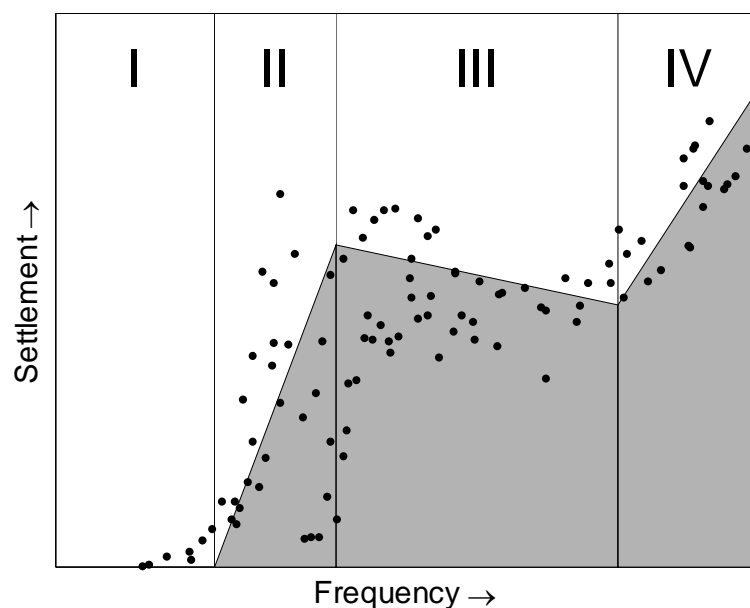

FIG. 12 – *Assignment of four frequency ranges, shown schematically together with measured data from the small-scale tests.*

operates at the higher end of Range III or the low end of Range IV, reducing f slightly to the lower end of Range III would have several advantages. Firstly, the compaction effect might increase to some extent. Secondly, lower f would increase the lifespan of the machine and decrease the power of the engine, which would decrease fuel consumption. The decreased consumption together with the more effective compaction could mean significant reductions in emissions. In conclusion, while the effect of lowering f is positive for reducing machine wear and emissions, the effect on the compaction efficiency depends on the current compaction frequency in relation to f_r. It is possible that the optimal operating frequency is somewhat above resonance. However, this has yet to be studied in full-scale tests.

Conclusions

Dry and wet sand was compacted in 105 unique small-scale tests using rotating eccentric mass oscillators. The following conclusions are drawn from this study:

- Investigation of frequency-dependent compaction of sand was made possible in the present small-scale tests.
- The tests showed less controllability and higher scatter in the results than previous tests but successfully imitated the dynamic-to-static load ratio of roller compaction.
- No heave could be observed and it is thus assumed that the displacement of soil during compaction was minimal.
- The presented method for calculating frequency response, considering strain-dependent soil properties, successfully predicted measured dynamic quantities.
- Measured displacement amplitude versus frequency and force amplitude versus frequency relationships agreed well with published literature.
- There is no single dynamic quantity that is governing for soil compaction, but rather a combination. Frequency has a substantial influence.
- Frequency-dependent compaction exhibits a local maximum around resonance, producing more efficient compaction close to this frequency. Well above resonance, increasing the frequency implies a higher degree of compaction.

The above results contain dynamic effects that need to be further investigated. Possible reasons for these effects are discussed above. It is desirable to fully understand these phenomena before studying the practical implications for roller compaction in full-scale tests. It is possible that roller compaction could be optimized

by adjusting the frequency with regard to compaction efficiency, emissions and lifespan of machine parts.

References

Adam, D., 1996., *Flächendeckende Dynamische Verdichtungskontrolle (FDVK) mit Vibrationswalzen* [Continuous Compaction Control with Vibratory Rollers], PhD thesis, University of Vienna, Vienna, Austria (in German).

Anderegg, R. and Kaufmann, K., 2004, "Intelligent Compaction with Vibratory Rollers," *Transportation Research Record. 1868*, Transportation Research Board, Washington, D.C., pp. 124–134.

Baidya, D. K. and Murali Krishna, G., 2001, "Investigation of Resonant Frequency and Amplitude of Vibrating Footing Resting on a Layered Soil System," *Geotech. Test. J.*, Vol. 24(4), pp. 409–417.

Bernhard, R. K., 1952, "Static and Dynamic Soil Compaction," *Highw. Res. Board, Proc. Annu. Meet.*, Vol. 31, pp. 563–592.

Converse, F. J., 1953, "Compaction of Sand at Resonant Frequency," *ASTM Spec. Tech. Publ. No. 156*, pp. 124–137.

D'Appolonia, D. J., Whitman, R. V. and D'Appolonia, E., 1969, "Sand Compaction with Vibratory Rollers," *J. Soil Mech. Found. Div.*, Vol. 95, No. 1, pp. 263–284.

Dobry, R. and Whitman, R. V., 1973, "Compaction of Sand on a Vertically Vibrating Table," *Evaluation of Relative Density and Its Role in Geotechnical Projects Involving Cohesionless Soils*, ASTM STP 523, ASTM International, West Conshohocken, PA, pp. 156–170.

Facas, N. W., Rinehart, R. V. and Mooney, M. A., 2011, "Development and Evaluation of Relative Compaction Specifications Using Roller-Based Measurements," *Geotech. Test. J.*, Vol. 34, No. 6, pp. 634–642.

Forssblad, L., 1980, "Compaction Meter on Vibrating Rollers for Improved Compaction Control," *Proceedings of International Conference on Compaction*, Vol.

2, Paris, France, April 22-24, 1980, Ecole Nationale des Ponts et Chaussées and Laboratoire Central des Ponts et Chaussées, pp. 541–546.

Gazetas G., 1983, "Analysis of Machine Foundation Vibrations: State-of-the-Art," *Int. J. Soil Dyn. Earthq. Eng.*, Vol. 2, No. 1, pp. 2-43.

Hardin, B. O. and Drnevich, V. P., 1972a, "Shear Modulus and Damping in Soils: Design Equations and Curves," *J. Soil Mech. Found. Div.*, Vol. 98, No. 7, pp. 667–692.

Hardin, B. O. and Drnevich, V. P., 1972b, "Shear Modulus and Damping in Soils: Measurement and Parameter Effects," *J. Soil Mech. Found. Div.*, Vol. 98, No. 6, pp. 603-624.

Lysmer, J. and Richart, F. E., Jr., 1966, "Dynamic Response of Footings to Vertical Loading," *J. Soil Mech. Found. Div.*, Vol. 92, No. 1, pp. 65–91.

Mandal, A. and Baidya, D. K., 2004, "Effect of Presence of Rigid Base within the Soil on the Dynamic Response of Rigid Surface Foundation," *Geotech. Test. J.*, Vol. 27, No. 5, pp. 475–482.

Mandal, A., Baidya, D. K. and Roy, D., 2012, "Dynamic Response of the Foundations Resting on a Two-layered Soil Underlain by a Rigid Layer," *Geotech. Geol. Eng.*, Vol. 30, Issue 4, pp. 775-786.

Massarsch, K. R., 2004, "Deformation Properties of Fine-Grained Soils from Seismic Tests," Keynote lecture*, Proceedings of the Second International Conference on Site Characterization*, ISC'2, Porto, Portugal, September 19-22, 2004, International Society of Soil Mechanics and Geotechnical Engineering, London, England, pp. 133–146.

Mooney, M. A. and Rinehart, R. V., 2009, "In Situ Soil Response to Vibratory Loading and Its Relationship to Roller-Measured Soil Stiffness," *J. Geotech. Geoenviron. Eng.*, Vol. 135, No. 8, pp. 1022–1031.

Richart, F. E. and Whitman, R. V., 1967, "Comparison of Footing Vibration Tests with Theory," *J. Soil Mech. Found. Div.*, Vol. 93, No. 6, pp. 143-168.

Rollins, K. M., Evans, M. D., Diehl, N. B. and Daily, W. D. III, 1998, "Shear Modulus and Damping Relationships for Gravels." *J. Geotech. Geoenviron. Eng.*, Vol. 124, No. 5, pp. 396–405.

Schnabel, P. B., Lysmer, J. and Seed, H. B., 1972, *SHAKE: a Computer Program for Earthquake Response Analysis of Horizontally Layered Sites*, Earthquake Engineering Research Center, University of California, Berkeley, 92 p.

Stokoe, K. H., II, Darendeli, M. B., Andrus, R. D., and Brown, L. T., 1999, "Dynamic soil properties: Laboratory, field and correlation Studies," *Proceedings of the Second*

International Conference on Earthquake Geotechnical Engineering, Vol. 3, Lisbon, Portugal, pp. 811–845.

Susante, P. J. and Mooney, M. A., 2008, "Capturing Nonlinear Vibratory Roller Compactor Behavior through Lumped Parameter Modeling," *J. Eng. Mech.*, Vol. 134, No. 8, pp. 684-693.

Thurner, H. and Sandström, Å., 1980, "A New Device for Instant Compaction Control," *Proceedings of International Conference on Compaction*, Vol. 2, Paris, France, April 22-24, 1980, Ecole Nationale des Ponts et Chaussées and Laboratoire Central des Ponts et Chaussées, pp. 611–614.

Vucetic, M. and Dobry, R., 1991, "Effect of Soil Plasticity on Cyclic Response," *J. Geotech. Engrg.*, Vol. 117, No. 1, pp. 89–107.

Wersäll, C. and Larsson, S., 2013, "Small-Scale Testing of Frequency-Dependent Compaction of Sand Using a Vertically Vibrating Plate," *Geotech. Test. J.*, Vol. 36, No. 3, pp. 1-10.

Yoo, T-S. and Selig, E. T., 1979, "Dynamics of Vibratory-Roller Compaction," *J. Geotech. Engrg. Div.*, Vol. 105, No. 10, pp. 1211–1231.